CODE DESIGN FOR ENERGY HARVESTING AND JOINT ENERGY AND INFORMATION TRANSFER USING RUN LENGTH LIMITED CODES

A THESIS SUBMITTED TO

THE GRADUATE SCHOOL OF ENGINEERING AND SCIENCE

OF BILKENT UNIVERSITY

IN PARTIAL FULFILLMENT OF THE REQUIREMENTS FOR

THE DEGREE OF

MASTER OF SCIENCE

IN

ELECTRICAL AND ELECTRONICS ENGINEERING

By

Mert Özateş

July 2018

Code Design for Energy Harvesting and Joint Energy and Information Transfer Using Run Length Limited Codes
By Mert Özateş
July 2018

We certify that we have read this thesis and that in our opinion it is fully adequate, in scope and in quality, as a thesis for the degree of Master of Science.

Tolga Mete Duman (Advisor)

Sinan Gezici

Ayşe Melda Yüksel Turgut

Approved for the Graduate School of Engineering and Science:

Ezhan Karaşan
Director of the Graduate School

ABSTRACT

CODE DESIGN FOR ENERGY HARVESTING AND JOINT ENERGY AND INFORMATION TRANSFER USING RUN LENGTH LIMITED CODES

Mert Özateş
M.S. in Electrical and Electronics Engineering
Advisor: Tolga Mete Duman
July 2018

Energy harvesting wireless networks and networks that benefit from wireless energy transfer have become popular in the last decade. In these networks, the users can obtain the required energy for transmission from an external source, which eliminates the need of battery replacement. Therefore, such networks have a high potential for applications in different areas including wireless sensor networks, wireless body networks and Internet of Things (IoT). While there have been many advancements for energy harvesting communications and joint energy and information transfer from information and communication theoretic perspectives in the literature, these subjects have not been studied from a practical coding and transmission point of view in depth.

With the above motivation, in this thesis, we propose a serially concatenated coding scheme to communicate over binary energy harvesting communication channels with additive white Gaussian noise (AWGN), and design explicit and implementable codes for both long and short block lengths. Run length limited (RLL) codes are used to induce the required nonuniform input distributions for both cases. We employ low density parity check (LDPC) codes for long block lengths, while for short block length designs, we utilize convolutional codes for error correction. We consider different decoding approaches for the two cases, i.e., an iterative decoder is used for the former while Bahl-Cocke-Jelinek-Raviv (BCJR) algorithm over the product trellis of the convolutional and run length limited codes is used for the latter. Also, by noticing that similar coding solutions can be employed, we extend our work to joint energy and information transfer for both scenarios. Numerical examples demonstrate that the newly optimized codes with an inner RLL code are superior to the point-to-point optimal codes

for AWGN channels for long block lengths when energy harvesting or joint energy and information transfer is considered, and that, for the short block length case, concatenated convolutional and RLL codes with higher minimum distances offer excellent performance.

Keywords: Energy harvesting, run length limited codes, low density parity-check codes, joint energy and information transfer, short block length codes, convolutional codes.

ÖZET

ENERJİ HASADI VE ORTAK ENERJİ VE BİLGİ TRANSFERİ İÇİN ÇALIŞMA UZUNLUĞU SINIRLI KODLARI KULLANARAK KOD DİZAYNI

Mert Özateş
Elektrik ve Elektronik Mühendisliği, Yüksek Lisans
Tez Danışmanı: Tolga Mete Duman
Temmuz 2018

Enerji hasadı gerçekleştiren veya kablosuz enerji transferinden yararlanan kablosuz ağlar son yıllarda giderek popüler hale gelmektedir. Bu ağlarda kullanıcılar iletim için gerekli enerjiyi dışarıdan bir kaynaktan elde ederler ve herhangi bir batarya yenilenmesine gerek kalmaz. Dolayısıyla, bu ağlar kablosuz sensör ağları, kablosuz beden ağları ve nesnelerin interneti dahil olmak üzere birçok alanda uygulamalar için önemli bir potansiyel teşkil etmektedir. Enerji hasadı ve ortak enerji ve bilgi transferi konusunda bilgi kuramı ve iletişim yönünde birçok gelişme olsa da, bu konular üzerinde pratik kodlama yönünde sınırlı sayıda çalışma yapılmıştır.

Bu tezde, toplamsal beyaz Gaussian gürültülü (AWGN) ikili enerji hasadı iletişim kanalları üzerinde haberleşme amacıyla seri sıralanmış bir kodlama şeması öneriyoruz ve uzun ve kısa blok uzunluklarında açık ve uygulanabilir kodlar dizayn ediyoruz. Uzun ve kısa kodların her ikisi için de gerekli doğrusal olmayan girdi dağılımını elde etmek için çalışma uzunluğu sınırlı (RLL) kodları kullanıyoruz. Blok uzunluğu yüksek kodlar için düşük yoğunluklu parite kontrol (LDPC) kodları, kısa blok uzunluklu kodlar içinse kıvrımlı kodları dışsal hata düzeltici kod olarak kullanıyoruz. Kodçözme yöntemi olarak yüksek blok uzunluklu kodlar için yinelemeli bir kodçözücü kullanırken, düşük blok uzunluklu kodlarda kıvrımlı ve RLL kodların birleşimi için Bahl-Cocke-Jelinek-Raviv (BCJR) algoritmasından yararlanıyoruz. Bunun yanında, enerji hasadı için yaptığımız çalışmaları benzer kodlama şemalarının kullanılabilmesi sebebiyle ortak enerji ve bilgi transferi konusunda genişletiyoruz. Sayısal örnekler yüksek blok uzunluklu kodlarda içsel bir RLL kodla beraber optimize edilen yeni kodların standart AWGN kanalları için optimize edilmiş kodlara göre yüksek performans sağladığını,

düşük blok uzunluklu kodlarda ise yüksek asgari uzunluğa sahip birleşik kıvrımlı ve RLL kodların yüksek performans gösterdiğini göstermiştir.

Anahtar sözcükler: Enerji hasadı, düşük yoğunluklu parite kontrol kodları, ortak enerji ve bilgi transferi, kısa blok uzunluklu kodlar, kıvrımlı kodlar.

Acknowledgement

First and foremost, I would like to thank my advisor, Prof. Tolga Mete Duman for his continuous support and patience throughout my M.S. study. His deep knowledge and dedication for research have been a great importance for me.

I would also like to thank Prof. Sinan Gezici and Assoc. Prof. Ayşe Melda Yüksel Turgut as my examining committee members and for providing valuable comments.

I would like to thank my friend and colleague Mehdi Dabirnia for our valuable discussions, which help me a lot in the progress of my research.

I would also like to thank my office mates Sina Rezaei Aghdam, Mahdi Shakiba Herfeh, Ersin Yar, Umut Demirhan, Nurullah Karakoç, Talha Akyıldız, Büşra Tegin, and my other friends at Bilkent (especially my friends at Bilkent Chess Society) for my great memories.

Last, but not least, I would like to express my gratitude to my family for their love, support and motivation.

Contents

List of Figures

Abbreviations

AWGN	additive white Gaussian noise
BCJR	Bahl-Cocke-Jelinek-Raviv
BEC	binary erasure channel
BEHC	binary energy harvesting channel
BSC	binary symmetric channel
CCC	constant composition codes
CND	check node decoder
CSCC	constant subblock-composition codes
DMC	discrete memoryless channel
EMU	energy management unit
EXIT	extrinsic information transfer
FIFO	first-input first-output
ID	information decoding
i.i.d.	independent and identically distributed
IoT	Internet of Things
LDPC	low density parity check
LLR	log-likelihood ratio
MAC	medium access control

MANET mobile ad hoc network

MISO multiple-input single-output

MIMO multiple-input multiple-output

NLTC nonlinear trellis code

P2P point-to-point

RF radio frequency

RLL run length limited

SECC subblock energy-constrained codes

SNR signal-to-noise ratio

SWIPT simultaneous wireless information and power transfer

TDMA time-division multiple-access

VND variable node decoder

Chapter 1

Introduction

1.1 Overview

In energy harvesting wireless networks and networks that exploit wireless energy transfer techniques, wireless devices can harvest energy from nature or man-made sources (e.g., radio frequency (RF) signals) for their information transmission and processing, which eliminates the requirement of excessive energy storage in hardware and increases the network lifetime. Hence, such wireless networks have a high potential for applications in various areas including wireless sensor networks, wireless body networks and Internet of Things (IoT) [1], [2], and they have been enjoying an upsurge of interest in recent years.

Energy harvesting communication systems and joint energy and information transfer have been extensively studied from an information theoretic perspective in the literature. For energy harvesting communications, capacity bounds for different channel models including noiseless and additive white Gaussian noise (AWGN) channels are computed for no battery, finite-sized battery and infinite-sized battery cases [3, 4, 5, 6]. For joint energy and information transfer, Varshney demonstrates that there is a natural trade-off between the transmitted energy and the information rate, and there is a unique capacity achieving input distribution

in [7]. Despite these information theoretic works, research considering practical code design for energy harvesting communication systems and joint energy and information transfer is limited, which motivates this thesis.

We consider design of practical codes based on a serially concatenated coding scheme with an inner run length limited (RLL) code and an outer error correction code for energy harvesting communication systems and joint energy and information transfer. In both energy harvesting and joint energy and information transfer, a nonuniform input distribution is required for optimal transmission. On the other hand, classical linear block or convolutional codes induce a uniform distribution of zeros and ones at the channel input, and they are not suitable for direct use. Hence, in this thesis, we utilize RLL codes [8] to obtain the required nonuniform input distribution for both scenarios. RLL codes are represented by two parameters d and k, where d and k denote the allowable minimum and maximum number of zeros between consecutive ones, respectively, therefore they are suitable to regulate the energy usage at the transmitter as well as power transfer via RF signals. In the existing literature, RLL codes have been mostly used for optical and magnetic recording for disk drives or visible light communications. However, here we consider their use as inner codes for our proposed coding scheme.

1.2 Thesis Contributions

The main contribution of this thesis is design of explicit and implementable codes to communicate over noisy binary energy harvesting systems and to transmit energy and information simultaneously. We propose a serially concatenated coding scheme for energy harvesting communications for long block lengths, where an inner RLL code generates the required nonuniform input distribution for optimal transmission and an outer low density parity check (LDPC) code provides error correction capabilities. At the receiver side, we employ an iterative decoder with two decoding approaches with different complexities. The simplified approach ignores the memory in the channel state while the improved decoding solution

exploits this memory by considering it jointly with the code trellis, i.e., via an extended trellis. For code design purposes, we fix the inner RLL code and optimize the outer LDPC code using Extrinsic Information Transfer (EXIT) charts and a random perturbation technique. Via numerical examples, we demonstrate that the newly optimized codes with an inner RLL code outperform the off-the-shelf codes (i.e., codes optimized for standard point-to-point (P2P) AWGN channels) and improved decoding solution is superior to the simplified one.

We also extend our work for energy harvesting communications to joint energy and information transfer since it is a highly related problem that can exploit similar coding approaches. In joint energy and information transfer, the purpose is to increase the transmitted power levels and information rates at the same time, however, there is a natural trade-off between the two. We consider on-off signalling to model this trade-off and exploit the serially concatenated coding scheme that we propose for energy harvesting communications with small modifications. We design the outer LDPC code using techniques as in the energy harvesting case, and demonstrate via numerical examples that the newly designed codes are superior to the P2P optimal codes.

In our setup, nonlinear trellis codes (NLTCs) can also be used as inner codes as done in [9] and [10]. However, in this thesis, we utilize the RLL codes as they allow for higher transmission rates for both energy harvesting and joint energy and information transfer. We also note that the results in this thesis are based on 2-state RLL codes, which are very simple compared to the existing solutions.

We also address short block length code designs for energy harvesting communications and joint energy and information transfer with the motivation that long block length codes are not suitable for communication systems with stringent delay and complexity constraints. In this case, we propose a serially concatenated coding scheme with an inner RLL and an outer convolutional code, and describe the concatenated code by a product trellis. We perform decoding via Bahl-Cocke-Jelinek-Raviv (BCJR) algorithm over the product trellis at the receiver side, and aim to maximize the minimum free distance of the concatenated code for code design purposes. Through several numerical examples, we demonstrate that the

concatenated convolutional and RLL codes with higher minimum distances offer superior performance.

1.3 Thesis Outline

The rest of the thesis is organized as follows. In Chapter 2, the existing literature about the capacity bounds and practical coding approaches for energy harvesting communications and joint wireless energy and information transfer are reviewed. In Chapter 3, we describe the proposed coding scheme for energy harvesting communication systems, and design explicit and implementable codes for that scenario. In Chapter 4, we extend our work to code design for joint energy and information transfer. In Chapter 5, we focus on design of short block length codes for the two scenarios under consideration. We conclude the thesis and highlight some future research directions in Chapter 6.

Chapter 2

Literature Review

In this chapter, we review the prior works that approach energy harvesting communication systems and joint energy and information transfer from information and communication theoretic perspectives, and the previous literature that develop practical coding solutions for these scenarios.

The chapter is organized as follows. In Sections 2.1 and 2.2, prior works on energy harvesting communication systems and joint energy and information transfer are reviewed, respectively. The existing literature on practical coding solutions to these problems is the focus of Section 2.3, and finally the chapter is concluded in Section 2.4.

2.1 Energy Harvesting Communication Systems

In energy harvesting communication systems, the transmitter obtains the required energy for transmission from an external source [3], as depicted in Figure 2.1. For each channel use, the transmitter transmits a symbol and harvests a unit of energy with probability q, which denotes the energy arrival probability. Harvested energy is used for transmission or it is stored in a finite-sized battery (if a battery is equipped) if the transmission requires no energy. Transmitted symbol is constrained by the available energy, hence a zero symbol is transmitted regardless of what the input bit is in the case of energy shortage.

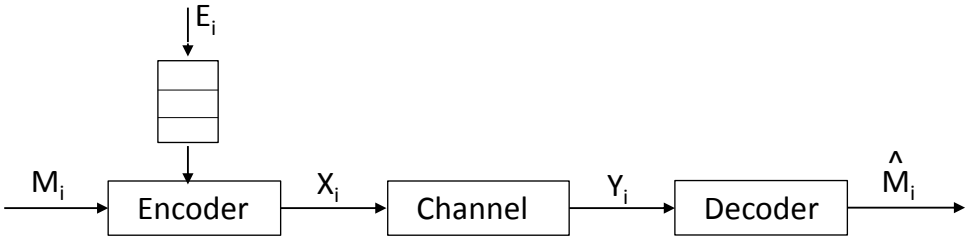

Figure 2.1: Block diagram of an energy harvesting communication system.

In most of the prior works about energy harvesting communication systems, the main purpose is to calculate bounds on the channel capacity and to derive optimal transmission strategies for different scenarios. For the simplest case, if the energy state of the transmitter is independent and identically distributed (i.i.d.) in time, Shannon strategy [11] is proved to be optimal for transmission. However, presence of battery introduces memory into the system. Namely, the energy state depends on the previous state, the current channel input and the battery size in addition to the harvested energy at the current time instant, making the problem highly complicated.

Energy harvesting communications over a noiseless channel with a unit-sized battery is studied in [3]. In order to exploit the memory in the channel state, the

binary energy harvesting channel (BEHC) is modelled as an equivalent timing channel. In that model, after sending a "1" symbol, the encoder waits until a unit of energy is harvested to send another "1", and this idle time is denoted as Z_k, which has a geometric distribution with parameter q. After a unit of energy is harvested, the encoder waits a number of channel uses V_k according to Z_k and then transmits a "1". Encoder observes the idle time and the past channel inputs to calculate the state sequence, and decoder observes T_k, which denotes the number of channel uses between the $(k-1)$-th moment that the channel output $Y = 1$ and the k-th moment that $Y = 1$ to calculate the output sequence. The capacity of this channel is equal to the capacity of the BEHC, and it can be calculated as follows:

$$C_T = \sup_{p(u),v(u,z)} \frac{I(U;T)}{E[T]} \tag{2.1}$$

where U is an auxiliary random variable with a countably infinite support, $p(u)$ is the probability mass function of U and $v(u,z)$ is a mapping from the auxiliary random variable U and state Z to the channel input V. In order to calculate the capacity, optimal distribution for U should be found, which makes the problem complicated. Therefore, two upper bounds for the capacity of BEHC are derived in [3]. The first one is a genie upper bound, which assumes the timing channel state Z_k is known at the receiver, resulting in

$$C_{UB}^{genie} = \max_{p\in[0,1]} \frac{qH_2(p)}{q+p(1-q)} \tag{2.2}$$

where $H_2(p)$ is the binary entropy function and p is the parameter of geometric random variable V, which denotes the number of channel inputs that encoder waits to transmit a "1" after a unit of energy is harvested.

The second upper bound is called the state leakage upper bound, which is obtained by measuring the minimum information carried by m-letter sequence

T^m about Z^m, which can be calculated as:

$$C_{UB}^{leakage} = \sup_{p_T(t)\in P} \frac{H(T) - \sum_{t=1}^{\infty} \frac{H_2((1-q)^t)}{1-(1-q)^t} p_T(t)}{E[T]} \tag{2.3}$$

where q is the energy arrival probability, $H_2(.)$ is the binary entropy function, T represents the differences between the channel uses for which "1"s are observed at the output of the channel, $p_T(t)$ is the probability density function of T, and P is given by

$$P = \left\{ p_T(t) \middle| \sum_{t=1}^{s} p_T(t) \leq 1 - (1-q)^s, s = 1, 2, .. \right\}. \tag{2.4}$$

Two extreme cases, i.e., infinite and no battery cases, are also studied in [3]. For the infinite-sized battery case, the capacity is given by

$$C_{IS} = \begin{cases} H_2(q) & q \leq \frac{1}{2}, \\ 1 & q > \frac{1}{2}. \end{cases} \tag{2.5}$$

If there is no energy storage, the harvest first model is considered rather than the transmit first model. In the harvest first model, energy is harvested and then the input symbol is transmitted through a BEHC. In this case, channel input $X_i = 1$ is allowed only if a unit of energy is harvested for that channel use, i.e., $E_i = 1$. Then, the channel capacity for this case can be calculated as follows:

$$C_{ZS} = \max_{p} H_2(pq) - pH_2(q). \tag{2.6}$$

Several capacity results and achievable rates are depicted in Figure 2.2.

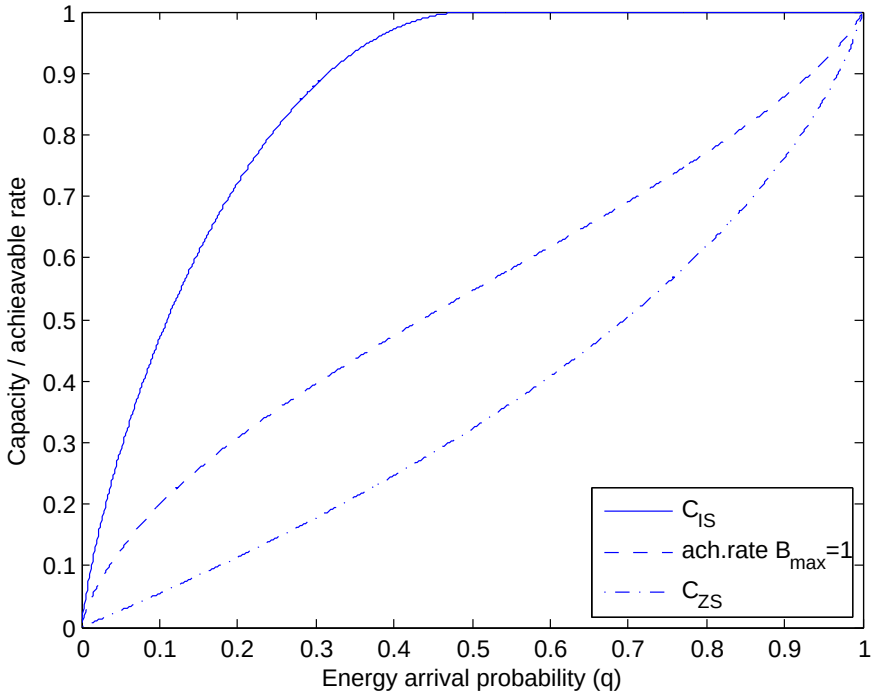

Figure 2.2: Capacity results for zero battery and infinite battery cases and achievable rates with unit battery.

Energy harvesting systems communicating over an AWGN channel with an infinite-sized battery is studied in [4]. In that work, a scalar AWGN channel is considered with input X, output Y and Gaussian noise with zero mean and unit variance. An external source supplies E_i units of energy at each channel use and the unused energy is stored in a battery with size $E_{max} = \infty$. Presence of the infinite-sized battery makes the probability of overflow zero. At the i-th channel use, E_i units of energy is supplied to the battery and X_i^2 amount of energy is dissipated from it, where X_i represents the channel input. Hence, the power constraint on channel input symbols is as follows:

$$\sum_{i=1}^{k} X_i^2 \leq \sum_{i=1}^{k} E_i, k = 1, ..., n. \tag{2.7}$$

In a standard AWGN channel an independent distribution of input symbols achieves the channel capacity as pointed out in [12]. However, the power constraint in (2.6) on the input symbols makes channel inputs dependent to past channel inputs, hence the problem requires finding the capacity of channels with memory. An upper bound on the capacity of this channel is equal to the capacity of a classical AWGN channel with an average power constraint P equalling the energy arrival rate, which can be calculated as

$$C = \frac{1}{2} log(1 + P). \tag{2.8}$$

Since the battery is infinite-sized, this capacity can be achieved by the two transmission policies proposed in [4], which are save-and-transmit and best-effort-transmit schemes. In the save-and-transmit scheme, the main idea is splitting the transmission into two phases, collecting sufficient amount of energy in the first phase (saving phase), and then transmitting data in the second phase (transmitting phase). By following the notation in [4], if the length of the saving phase is $h(n)$ channel uses, and the length of the transmitting phase is $n - h(n)$ channel uses, the AWGN channel capacity can be achieved by letting $h(n)$ and $n - h(n)$ to go to infinity since an unbounded amount energy is stored in the saving phase making the probability of energy shortage in the transmitting phase zero. In the best-effort-transmit scheme, there is no saving phase and data is transmitted directly. If there is available energy in the battery, the corresponding code symbol is sent and a zero symbol is sent otherwise. The number of mismatches between the codebook and the transmitted data due to energy shortage is finite from the strong law of large numbers, hence the classical AWGN channel capacity in (2.8) can be achieved.

Authors of [5] study communication over the classical AWGN channel where the channel input is amplitude-constrained and stochastically varies at each channel use, which is equivalent to the problem of binary energy harvesting communications over an AWGN channel with no battery for energy storage. Prior to that

work, Smith determined the capacity achieving input distribution for a static amplitude constrained AWGN channel in [13] and Shannon derived the capacity of a state-dependent channel whose state information is available only at the transmitter in [11]. Authors of [5] combine these two prior works, and they obtain the capacity of a time-varying amplitude constrained channel by the Shannon strategy and they optimize the input distribution of the extended alphabet channel (extended according to the amplitude constraints). Their results show that the capacity of AWGN channels with time-varying input amplitude constraints is given by

$$C = \max_{F \in \Omega} I_F(T;Y), \tag{2.9}$$

where $T = [T_1, T_2]$ is a random vector that generates the codewords. T_1 and T_2 have support sets $[-a_1, a_1]$ and $[-a_2, a_2]$ with joint cumulative distribution function F. Authors demonstrate that the input distribution that achieves this capacity has a support set of finite cardinality.

If the battery is finite-sized, the problem of calculating the exact channel capacity is still open. However, bounds on the channel capacity for this case are studied in [6]. There is also a recent paper [14] that covers the capacity analysis of a discrete energy harvesting channel with a finite-sized battery using a general framework.

Energy harvesting wireless sensor networks where one sensor communicates with a single receiver are studied in [15]. In that work, the energy harvesting sensor performs source acquisition and data transmission over a time-varying channel. At each time slot k, E_k amount of energy is harvested and stored in an infinite-sized battery. After that, X_k number of bits are generated by the source encoder. Number of generated bits depends on the distortion level and energy per channel use allocated to source encoder and observation state. This bit stream is buffered into a first-input-first-output (FIFO) queue first and then transmitted through a fading channel, which is driven by a stationary ergodic process H_k.

The main problem considered in [15] is finding the optimal policy for distribution of the harvested energy by the sensor between source acquisition and data transmission. An energy management unit (EMU) decides the allocation of the energy to source acquisition and data transmission based on the statistics of energy harvesting, data queue, fading channel SNR and measurement SNR, which is a characterization of source acquisition process. Performance of the system is evaluated according to the stability of the data queue under an average distortion constraint at the receiver, and it is demonstrated that the optimal policies require dividing the battery into two subcomponents which are used for source acquisition and data transmission. Allocating the available energy to these two subcomponents allows separate optimization of source acquisition and data transmission processes. Suboptimal strategies where either source acquisition or data transmission is optimized are also considered, and numerical results show that increasing the variance of energy harvesting process increases the distortion at the receiver and a joint optimization of source acquisition and data transmission rather than optimization of one of them provides significant gains.

Energy harvesting multi-hop sensor networks are studied in [16], where the correlations among different sensor measurements are exploited via distributed source coding. An online learning algorithm based on Lyapunov optimization with weight perturbation is proposed to perform joint optimization of source coding and data transmission. Numerical examples demonstrate that proposed strategy approaches optimality in terms of average network cost. Communication over a fading channel with an energy harvesting sensor is studied in [17], where a delay constraint is also imposed on the system and optimal strategies for compression and transmission are derived.

Design and analysis of the conventional medium access control (MAC) protocols including time-division multiple-access (TDMA), framed-ALOHA (FA) and dynamic-FA (DFA) for energy harvesting wireless sensor networks are studied in [18]. In the communication scheme considered, there are multiple energy harvesting devices transmitting their data in periodic inventory rounds (IR). The transmitted data is collected at a fusion center (FC), and energy harvesting is performed between two successive IRs. Two metrics are introduced and derived for

each MAC protocol to measure the performance of the protocols, which demonstrate delivery efficiency and time efficiency. In addition, a backlog estimation algorithm is proposed for the DFA protocol. Detailed information about the DFA protocol can also be found in [19].

In addition to the above, optimal transmission and scheduling policies for several scenarios in energy harvesting communication systems are studied in the literature. Optimal power allocation policies for throughput maximization where causal state information (SI) or full SI of energy harvesting channel is available is studied in [20], and a dynamic programming approach is considered to solve the optimization problem. Optimal transmission policies for communication over a fading channel are studied in [21]. A directional water-filling algorithm is proposed to maximize the throughput and minimize the completion time of communication session subject to the finite-sized battery and causality constraints, which means that energy flow can only be from past to future and cannot exceed the battery size. An optimal scheduling policy that represents an iterative block coordinate ascent algorithm based on convex optimization for a multi-input multi-output (MIMO) multi-access channel is proposed in [22]. Authors of [23] consider the scenario with data packets having different importance values. The transmitter has to decide whether it should transmit the packet or not by considering the importance of the packet, the channel state and harvested energy. In that work, two approaches are proposed to solve the transmission problem; one is based on a function approximation and the other one uses reinforcement learning. Energy harvesting communications where the knowledge of the amount of available energy in the subsequent time instance is not available and only the statistical distribution of energy arrivals is known is examined in [24]. Authors of [25] consider remote estimation with an energy harvesting sensor and derive the optimal power allocation strategies for that scenario. Also, performance bounds of the considered scenario in [25] are derived in [26]. Optimal offline and online transmission policies with energy harvesting relays to maximize the end-to-end system throughput subject to the data buffer size and energy storage constraints are studied in [27]. Authors of [28] propose an energy-aware transmission policy with the objective of maximizing long-term average throughput where the

finite-sized battery usage is constrained, and they demonstrate that the proposed strategy is asymptotically optimal if the battery has sufficient capacity.

Large scale networks, particularly mobile ad hoc networks (MANETs) and cellular networks with energy harvesting are also considered in a few works in the literature. MANETs are studied in [29], where the transmitters are distributed according to a homogenous Poisson point process and transmission power is optimized with the constraints on the throughput and outage probability. On the other hand, authors of [30] study cellular networks, by assuming transmitters are distributed as in [29] and modelling the energy field using stochastic geometry to design large-scale energy harvesting wireless networks.

2.2 Joint Energy and Information Transfer

Simultaneous energy and information transmission is a highly related problem to energy harvesting. Here the purpose is to increase the transmitted energy levels as well as to achieve reliable communication. On the other hand, there is a natural trade-off between the transmitted energy and information, for which the first explicit formulation is provided in [7]. The fact emphasized in [7] is that to maximize the transmitted energy, the most energetic symbol should be sent all the time and to maximize the transmitted information, a different capacity-achieving input distribution should be used. These two objectives can be stated as an optimization problem where information rate is maximized under a minimum received energy constraint. If $X_1^n = (X_1,X_2,...,X_n)$ denotes the channel input, $Y_1^n = (Y_1,Y_2,...,Y_n)$ denotes the channel output and B denotes the minimum received energy, the n-th capacity-energy function is computed as follows:

$$C_n(B) = \max_{X_1^n : E[b(Y_1^n)] \geq nB} I(X_1^n; Y_1^n). \tag{2.10}$$

Here, the input vector X_1^n that satisfies the condition $E[b(Y_1^n)] \geq nB$ is called a B-admissible test source and the maximization is over the B-admissible test

sources. Then, the capacity-energy function of the channel is given by

$$C(B) = \sup_n \frac{1}{n} C_n(B). \tag{2.11}$$

A coding theorem, which provides an operational significance to (2.12) can be proven. Some properties of the capacity-energy function have also been developed in [7].

Interactive exchange of energy and information is studied in [31]. In that work, a system model that includes two nodes communicating with on-off signalling is considered. At each channel use k, node j transmits an energy-carrying symbol (on-symbol) $X_{j,k} = 1$ or an off-symbol ($X_{j,k} = 0$). Transmission of an "on" symbol costs one unit of energy to the sender node and transmission of an "off" symbol requires no energy use. Therefore, a node can transmit a zero only if there is no available energy in that node. Since the channel is noiseless, the transmitted symbol is directly received from the recipient node. Transmission of an "on" symbol implies that one unit of energy is transferred from the sender to the recipient, therefore the energy state of node j evolves as:

$$U_{1,k} = (U_{1,k-1} - X_{1,k-1}) + X_{2,k-1} \tag{2.12}$$

where the total number of energy units in the two nodes is set to a finite number U, the initial state is set as $U_{1,1} = u_{1,1} \leq U$, and in the channel use k, $U_{2,k} = U - U_{1,k}$. Therefore, the coding strategies that aim to maximize the information rate alone are not optimal for this scheme since the energy is constrained and the energy flow should jointly be considered with the information flow for optimal transmission.

The coding strategy proposed in [31] is based on codebook multiplexing. That is, each node constructs U codebooks and the codebooks used for transmission are chosen according to the energy state of the node. Namely, if a node has a large amount of energy, a codebook that includes a larger fraction of ones is utilized, and if the amount of the available energy units is low, a codebook

with a larger fraction of zeros is used. If the construction of the codebooks is independent, an inner capacity bound can be achieved and if the codebooks are jointly constructed, outer bounds on the capacity are obtained. Simulation results demonstrate that using adaptive codebooks that consider energy state of the nodes provide significant gains over random codebooks in terms of achievable sum-rates. Extensions to the stochastic evolution of energy harvesting at the recipient node and transmission over noisy channels can also be found in [31].

Simultaneous wireless information and power transfer (SWIPT) is also studied for various models in the literature. The fundamental trade-off between the transmitted energy and information rate formulated in [7] is studied for a frequency-selective AWGN channel in [32]. Practical receiver implementations including separate and integrated information and energy receivers along with rate-energy characterizations are studied in [33], and optimal transmission strategies to achieve different rate-energy trade-offs are derived for both implementations. Authors of [33] also consider the same framework for MIMO broadcast channels in [34]. Optimal beamforming design for a multiuser multiple-input single-output (MISO) SWIPT system is studied with the purpose of maximizing weighted sum-power at the energy harvesting receivers subject to a signal-to-interference-and-noise ratio (SINR) constraint at information decoding receivers in [35]. Authors of [36] consider a resource allocation problem for a SWIPT orthogonal frequency-division multiple access (OFDMA) system and they propose a non-linear energy harvesting model in order to increase the power conversion efficiency at the receiver. Linear precoder design with the purpose of minimizing the minimum mean-square error (MMSE) for the SWIPT systems employing transmitters with hardware impairments is investigated in [37]. The case of opportunistic energy harvesting, where the receiver can perform either information decoding (ID) or energy harvesting (EH) at each time instance is studied in [38], and optimal mode switching policies between ID and EH are derived for flat-fading channels. Two-user MIMO interference channels are studied in [39] in the same context, and optimal transmission strategies are presented. Various power allocation strategies for a wireless cooperative network communicating over a relay are proposed in [40]. Linear precoder design for MIMO interference channels

is studied in [41] with the objective of minimizing the average mean-square error under a harvested energy constraint at the receiver. Authors of [42] consider a Rician fading channel for the MIMO setup and propose two different strategies with the same purpose in [41]. MIMO wiretap channel is considered in [43], where the objective is to design the transmit covariance matrix to maximize the secrecy rate with the constraint on the harvested energy. As a very recent work, the problem of joint mode switching (between information decoding and energy harvesting) and power allocation is studied in [44], where the purpose is to maximize the harvested energy at the receiver under the constraints on the information rate and transmit power.

2.3 Practical Coding Schemes for Energy Harvesting and SWIPT

Energy harvesting and simultaneous information and energy transfer are studied from a communication theoretic perspective in a few recent papers as well. The authors in [9] focus on practical code design for joint energy and information transfer using on-off signalling over an AWGN channel. It is known that the optimal input distribution to maximize the transmitted information is a uniform distribution for the considered channel. However, in order to transmit more energy, a larger fraction of ones should be transmitted, hence a serially concatenated coding scheme that consists of an inner nonlinear trellis code (NLTC) and outer LDPC code is proposed. The inner NLTC is used to obtain the non-uniform input distribution, and the outer LDPC code ensures error correction. At the receiver side, an iterative decoding approach is considered, i.e., the receiver is divided into two subblocks and decoding is performed by exchanging of the extrinsic LLRs of the input symbols between these two subblocks.

In [9], the inner NLTC is designed with the goal of maximizing the minimum Hamming distance between the codewords on the trellis while satisfying an

average ones density in the codewords. In order to achieve this goal, set partitioning is performed to a selected subset of binary labels, for which minimum pairwise Hamming distance is maximized first, and then groups of two pairs are taken to maximize the minimum Hamming distance, and partitioning continues in this manner. Resulting output labels are assigned to branches by exploiting an extended Ungerboeck's rule to complete the NLTC design. For the design of the outer LDPC code, NLTC is fixed and EXIT chart analysis is utilized. Degree distributions of the LDPC codes are optimized using the random perturbation algorithm introduced in [45]. Simulation results demonstrate that optimized LDPC codes for the inner NLTC provide significant gains in terms of the bit error rate performance compared to both regular and irregular LDPC codes optimized for AWGN channels.

Practical code design based on a serial concatenation of an inner NLTC and an outer LDPC code to communicate over a binary energy harvesting channel with AWGN is studied in [10]. In that work, the energy harvesting transmitter includes a finite-sized battery and energy arrivals are modelled as a Bernoulli(q) process. At the receiver side, an iterative decoder is employed with two decoding approaches. The inner NLTC design and the outer LDPC code optimization are performed with the same approach used in [9]. Numerical results demonstrate the superiority of the designed codes compared to the reference schemes, and the superiority of the proposed improved decoding method compared to the simplified decoding approach.

Code design for joint information and energy transfer using constrained RLL codes over a P2P communication link is studied in [49]. An RLL code is specified with two parameters d and k, which states that the number of zeros between two consecutive ones is at least d and at most k (the first and last sequences of zeros can be shorter than d in length). A type-1 RLL code is defined in the same way with a type-0 RLL code, however, d and k denote the number of ones between consecutive zeros. The system model considered in [49] consists of a transmitter, a P2P channel and a receiver. In the transmitter, the message sequence M is encoded by an RLL encoder into the sequence X^n, for which $X_i = 1$ denotes an

energy-carrying ("on") symbol and $X_i = 0$ denotes an "off" symbol. In the point-to-point channel, the energy is lost with a probability of p_{10}. At the receiver side, the received symbol is utilized for both decoding and energy harvesting. At the channel use i, the symbol Y_i is received; and, if $Y_i = 1$, the energy of the received symbol is stored in a supercapacitor. Energy utilization at the receiver is modelled stochastically; if $Z_i = 1$, a unit of energy is utilized from the supercapacitor or if the supercapacitor is empty, from the battery. If the energy is received but not used in the i-th channel use, i.e., $Z_i = 0$, it is stored in a battery with size B_{max}. The energy contained in the battery is denoted as B_i and it evolves as:

$$B_{i+1} = \min(B_{max}, (B_i + Y_i - Z_i)). \tag{2.13}$$

Since the battery is finite-sized, overflow and underflow events occur. In the case where the receiver harvests a unit of energy when the battery is full and the harvested energy is not used, an overflow event occurs. A random process O_i keeps track of the overflow events, $O_i = 1$ if $B_i = B_{max}$, $Y_i = 1$ and $Z_i = 0$ and $O_i = 0$ otherwise. Probability of an overflow event is defined as:

$$Pr(O) = \lim_{n\to\infty} \sup \frac{1}{n} \sum_{i=1}^{n} E[O_i]. \tag{2.14}$$

An underflow event takes place if the battery is empty, no energy is harvested and an energy unit is requested from the receiver. A random process U_i keeps track of the underflow events, $U_i = 1$ if $B_i = 0$, $Y_i = 0$ and $Z_i = 1$ and $U_i = 0$ otherwise. Probability of an underflow event is defined as:

$$Pr(U) = \lim_{n\to\infty} \sup \frac{1}{n} \sum_{i=1}^{n} E[U_i]. \tag{2.15}$$

The optimization problem in [49] is defined as minimizing the maximum underflow or overflow probabilities with reliable communication at a fixed rate R.

As a result, the code performance is evaluated according to the overflow and underflow probabilities at the receiver. Performance comparison of unconstrained codes and different RLL codes illustrates that by a proper choice of the RLL code parameters (d, k), they provide significant performance gains since the code structure can match to receiver's energy utilization model.

Authors of [50] study the scenario that the receiver completely relies on the received signal energy to satisfy its power requirements. They consider on-off signalling, where a "1" corresponds to an energy-carrying symbol and the transmitter sends only the codewords that have sufficient energy. In particular the codewords should include at least d ones in a window of $d+1$ bits. This constraint defines a type-1 (d, ∞) RLL code.

The problem of finding the capacity of a (d, ∞) code over a noiseless channel is first studied by Shannon and it is given by

$$C_0 = \lim_{N \to \infty} \frac{log_2 M_N}{N} \tag{2.16}$$

where M_N denotes the maximum number of distinct binary sequences of length N RLL codewords. RLL codes are characterized by Markov chains and a type-1 (d, ∞) RLL code can be modelled by a Markov chain consisting $d+1$ states, where $S_n \in \{1, 2, ...d+1\}$ denotes the state and X_n denotes the input symbol. State transition from S_{n-1} to S_n generates the input bit X_n. If $S_n \in \{1, 2, ...d\}$, a "1" is produced with probability 1, if $S_n = d+1$, a "0" is produced with probability p (which makes $S_{n+1} = 1$), and a "1" is produced with probability $1-p$ (which makes $S_{n+1} = d+1$). Since this is an irreducible and aperiodic Markov chain, the state transition probabilities π_j can be explicitly computed and the information rate is given by

$$R(p) = \pi_d H(p). \tag{2.17}$$

In [50], it is shown that (d, ∞) code capacity can be achieved by this Markov

chain with an optimal choice of the transition probability p. For a given d, (d, ∞) code capacity can be formulated as follows:

$$C_0 = \max_{0 \leq p \leq 1} R(p). \tag{2.18}$$

The problem of computing the achievable rates over memoryless channels using (d, ∞) codes is also studied in [50]. In general, the channel capacity is calculated as follows:

$$C = \lim_{N \to \infty} \sup_{P(X^N)} \frac{I(X^N; Y^N)}{N} \tag{2.19}$$

$$= \lim_{N \to \infty} \sup_{P(S^N)} \frac{I(S^N; Y^N)}{N} \tag{2.20}$$

where X^N denotes the input sequence, Y^N denotes the output sequence and S^N denotes the state sequence. Although (2.21) provides an expression for the channel capacity for the noiseless case, it is difficult to obtain the exact channel capacity for noisy channels and lower bounds are computed through numerical optimization or approximations. In general, a lower bound on the capacity for a stationary Markovian source over a memoryless channel is given by

$$C_{LB} = \sup_{P(S_1, S_2)} I(S_2; Y_2 | S_1). \tag{2.21}$$

Closed form expressions for the lower bounds on the channel capacity using a (d, ∞) RLL code are computed for a binary symmetric channel (BSC), a Z-channel and a binary erasure channel (BEC) in [50], and several numerical results are provided. These results demonstrate that increasing the RLL code parameter d degrades the capacity, and state transition probability p should be optimized according to the channel characteristics as well as the RLL code parameter d. For the case of binary symmetric and Z-channels, the optimized value of p depends on

both the RLL code parameter d and channel parameter q, however, for the case of a BEC, the optimized value of p does not vary with the erasure probability, i.e., it is same with the noiseless case for a given d.

Using subblock energy-constrained codes (SECCs) when the received signal is used for both decoding and energy harvesting is studied in [51]. SECCs are a class of codes that satisfy a carried energy constraint in every subblock. Bounds for the capacity over a discrete memoryless channel (DMC) and error exponents are derived in [51]. Constant subblock-composition codes (CSCCs) for which all the subblocks have the same fixed composition and constant composition codes (CCCs) for which every codeword have the same composition are also studied.

In SECCs, the codewords are partitioned into length L subblocks and composition of each subblock satisfies the following constraint:

$$\sum_{x\in X} b(x)\frac{N_j(x)}{L} = \sum_{x\in X} b(x)P_j(x) \geq B \tag{2.22}$$

where $b(x)$ denotes the harvested energy when $x \in X$ is transmitted, B denotes the required energy per symbol, $N_j(x)$ is the number of the occurrences of x in the subblock j and $P_j(x) \equiv N_j(x)/L$ denotes the j-th subblock composition. The codewords of a SECC are in the form of $n = kL$, where n is the codeword length, k is the number of the subblocks and L is the fixed subblock length. Capacity of an SECC block code transmitted over a DMC $(W^L : A^k \to (Y^L)^k)$, which has an input alphabet $\mathcal{A}$ and output alphabet $\mathcal{Y}^L$, can be calculated as

$$C^L_{SECC}(B) = \max_{P_{X_1^L}:X_1^L\in\mathcal{A}} \frac{I(X_1^L;Y_1^L)}{L} \tag{2.23}$$

where distribution of the subblocks is maximized over the set $\mathcal{A}$. Here, the capacity-achieving input distribution can be found by using the Blahut-Arimoto algorithm [52], [53].

For a CSCC with subblock composition P and subblock length L transmitted over a DMC with the input alphabet $\mathcal{T}_P^L$ and the output alphabet $\mathcal{Y}^L$, the channel capacity can be computed as follows:

$$C_{CSCC}^{L}(P) = \max_{P_{X_1^L}: X_1^L \in \mathcal{T}_P^L} \frac{I(X_1^L; Y_1^L)}{L}. \tag{2.24}$$

Numerical results show that the capacity of a SECC is generally higher than that of CSCC, due to the flexibility of SECCs. Also, the capacity of SECCs increases with the subblock length L, since larger L values allows a more flexible choice of the code symbols in a subblock. In addition, $C_{CSCC}^{L}(B)$ increases as the receiver energy buffer size E_{max} increases.

An encoding strategy called exponential backoff strategy for binary energy harvesting channels with a finite-sized battery is presented in [54]. In that work, a proposed strategy based on modelling the power usage as a fixed fraction of the available energy in the battery is studied first for a noiseless channel and then the analysis is extended to the case of noisy channels. The authors also construct the corresponding decoder and evaluate the performance of the proposed strategy by comparing the achievable rates with the exponential back-off strategy and a uniform policy for the power allocation. Numerical results demonstrate that the proposed strategy outperforms the uniform policy for large values of the expected energy rate over time.

2.4 Chapter Summary

In this chapter, we reviewed the prior works on energy harvesting communication systems as well as those on joint energy and information transfer that approach these problems from information and communication theoretic perspectives and present practical transmission solutions. In Sections 2.1 and 2.2, we introduced the main system models and presented relevant information theoretic limits and

optimal transmission/scheduling strategies for several scenarios for energy harvesting communications and joint energy and information transfer while we discussed existing results on the practical coding schemes and code design in Section 2.3.

Chapter 3

Code Design for Energy Harvesting Communications

In this chapter, we consider a binary energy harvesting communication system over a noisy channel, and design explicit and implementable codes to communicate over this system. We propose a serially concatenated coding scheme with an inner RLL code and an outer LDPC code, where the inner RLL code is used to obtain the suitable nonuniform input distribution while the outer LDPC code provides error correction. We fix the inner RLL code and design the outer LDPC code based on an EXIT chart analysis. A random perturbation based algorithm is used to optimize the degree distributions of the LDPC code ensembles. Numerical examples demonstrate that the newly designed codes outperform the P2P optimal codes over AWGN channels for energy harvesting communication systems.

The rest of the chapter is organized as follows. In Section 3.1, we introduce the system model. In Section 3.2, we describe the proposed coding approach and the corresponding decoder. In Section 3.3, we describe the design procedure for the LDPC code ensembles. We present several code design examples in Section 3.4, and conclude the chapter in Section 3.5.

3.1 System Model

We consider an energy harvesting communication system as depicted in Figure 3.1 where the transmitter is equipped with a finite-sized battery and the energy harvesting process is driven by an external source [3]. Energy arrivals are binary ($E_i \in \{0, 1\}$) and are modelled as an i.i.d. Bernoulli(q) random variables where q denotes the energy arrival probability in each time interval. The channel inputs are binary ($X_i \in \{0, 1\}$) as well. We assume that transmission of the bit "1" costs one unit of energy, while the bit "0" costs no energy. We consider on-off signalling, and denote the ones density of the channel input as p, i.e., $P(X_i = 1) = p$.

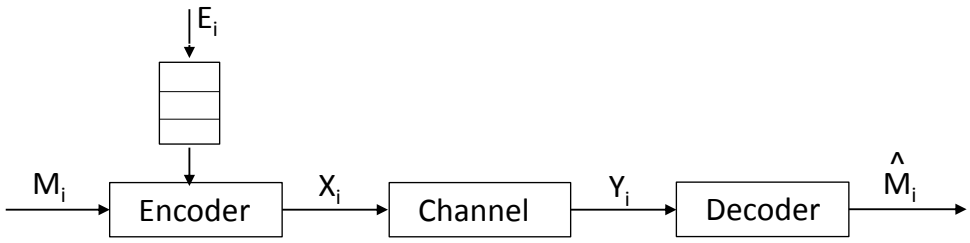

Figure 3.1: Block diagram of an energy harvesting communication system.

At each channel use i, a binary symbol X_i is transmitted and then E_i amount of energy is harvested. Harvested energy is stored for subsequent transmissions in a battery with capacity B_{max} if it is not full. The channel input X_i is constrained by the available energy in the battery. If there is no stored energy, a zero symbol is transmitted regardless of the input bit. Battery state at time instance i is denoted by S_i and it evolves as:

$$S_{i+1} = min\{S_i - X_i + E_i, B_{max}\}. \tag{3.1}$$

At the receiver side (which is explained in detail in Section 3.2), an iterative decoder adapted to the binary energy harvesting channel by using the zero-state stationary probability of the battery (π_0) is employed as a simplified decoding

approach. As an improved decoding solution, the energy state of the battery is incorporated into the RLL code trellis as well. We use the result from [10], where the battery state evolution is modelled as a Markov chain, and its zero-state stationary probability is calculated as

$$P(S=0) = \pi_0 = \frac{(1-q)p}{(1-q)p + q\sum_{i=0}^{B_{max}-1}(q/p)^i}. \tag{3.2}$$

Achievable rates for energy harvesting communications over an AWGN channel with noise variance σ^2 and a BSC with crossover probability ϵ are calculated in [10]. These rates depend on the parameter π_0, and the dependence of π_0 to the ones density of the input distribution indicates that the optimal ones density at the input is non-uniform, in general. Therefore, classical linear block or convolutional codes, which induce a uniform density of ones and zeros, cannot be directly utilized for optimal transmission. Here, we propose the use of RLL codes as inner codes, which induce a nonuniform distribution at the channel input, along with the outer LDPC codes for error correction.

3.2 Concatenation of LDPC and RLL Codes

In the proposed coding scheme for energy harvesting communication systems, the transmitter side consists of a serial concatenation of an LDPC encoder and inner RLL encoder as depicted in Figure 3.2. The LDPC coded sequence is encoded with an RLL encoder according to a (d, k) constraint where d and k denote the allowable minimum and maximum number of zeros between consecutive ones, respectively. Clearly, the parameters d and k regulate the ones density at the output of the RLL encoder. If the LDPC code has a rate R_1 and the RLL code has a rate R_2, the overall code rate of the communication scheme is R_1R_2.

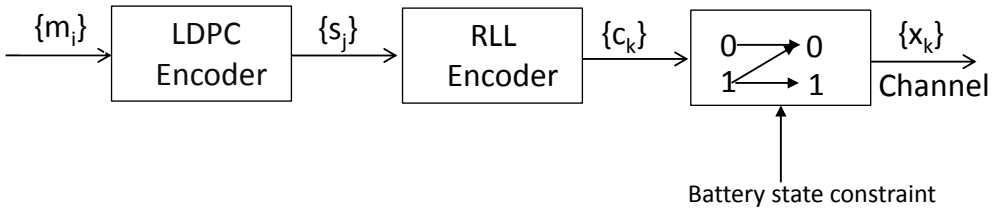

Figure 3.2: Block diagram of the transmitter.

At the receiver side, we employ an iterative decoder as depicted in Figure 3.3. The receiver consists of two blocks denoted as Block A and Block B, where Block A includes a BCJR decoder (RLL-BCJR) and the LDPC code's variable node decoder (VND). RLL-BCJR block computes a posteriori log-likelihood ratio (LLR) values of the binary symbols $\{s_j\}$ using channel observations and a priori information from the LDPC VND.

We first consider a simplified decoding approach to calculate the LLR values at the output of the RLL-BCJR block. Namely, we ignore the memory in the channel state and simply assume that the channel states are i.i.d., hence we have a memoryless Z-channel with $1 \rightarrow 0$ crossover probability π_0 connected to the AWGN channel. We match the RLL-BCJR block to this channel and calculate the LLR values at the output of the RLL-BCJR block as follows [46]:

$$L(u_l) = log\left[\frac{\sum\limits_{U^+} p(s_{l-1}=s', s_l=s, y)}{\sum\limits_{U^-} p(s_{l-1}=s', s_l=s, y)}\right], \tag{3.3}$$

$$p(s', s, y) = \alpha_{l-1}(s')\gamma_l^{mod}(s', s)\beta_l(s), \tag{3.4}$$

$$\gamma_l^{mod}(s', s) = \exp[u_k L^e(u_k)/2] \prod_{n=1}^{m} P(c_l^n = 1)\gamma_{l,1}^{mod} + P(c_l^n = 0)\gamma_{l,0}^{mod} \tag{3.5}$$

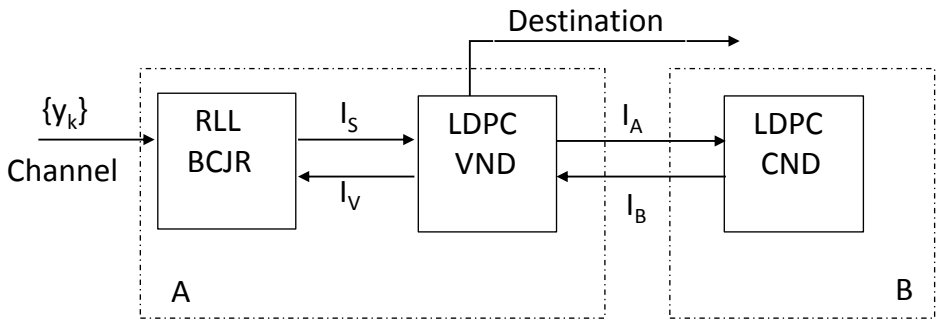

Figure 3.3: Block diagram of iterative decoder.

where s_l is the encoder state at time l, U^+ is the set of pairs (s', s) for the state transitions from state s' to state s with the encoder input $u_l = 0$ and U^- is the set of pairs (s', s) for the state transitions from state s' to state s with $u_l = 1$. c_l is the corresponding codeword output for the state transition (s', s), $L^e(u_k)$ is the a priori LLR of u_k, m is the length of the codeword output c_l, and $\gamma_{l,1}^{mod}$ and $\gamma_{l,0}^{mod}$ represent the state transition probabilities. These values are calculated using

$$\gamma_{l,1}^{mod} = \frac{1}{2\pi\sigma^2}\bigg((1-\pi_0)exp\Big(-\frac{(y_l^n - c_l^n)^2}{2\sigma^2}\Big) + \pi_0 exp\Big(-\frac{(y_l^n - 0)^2}{2\sigma^2}\Big)\bigg), \tag{3.6}$$

$$\gamma_{l,0}^{mod} = \frac{1}{2\pi\sigma^2}exp\Big(-\frac{(y_l^n - c_l^n)^2}{2\sigma^2}\Big). \tag{3.7}$$

Here n denotes the corresponding index of the channel observation y_l (or the corresponding codeword output c_l), and σ^2 is the noise variance.

As a second (improved) decoding approach, we implement the BCJR algorithm over an extended trellis, which includes the battery state as well. In this approach, there are $B_{max}+1$ states for each RLL code state, each one representing one battery state along with the RLL code state. This is similar to the approach taken in [10]. Note that we do not utilize this decoding approach for code design purposes due to its high complexity. Instead, we design the LDPC codes

with the simplified decoding approach above, and employ the specific codes from the designed ensembles to demonstrate the superiority of the improved decoding approach via finite block length simulations.

The LDPC VND computes the reliabilities of the binary symbols $\{s_j\}$ using a priori information from the RLL-BCJR algorithm and the information received from the LDPC check node decoder (CND) based on the code constraints. Block B consists of the LDPC CND that calculates the extrinsic LLR values of the binary symbols $\{s_j\}$ based on the a priori information received from the LDPC VND and the code constraints. Iterative decoding is performed by passing of the extrinsic information between Block A and Block B.

The overall decoding algorithm at the receiver is described as follows:

1. For initialization, the a priori LLRs of binary symbols $\{s_j\}$ at the input of Block A are set to zero.

2. A priori information for the RLL-BCJR is calculated by the LDPC VND by summing the incoming messages from the check nodes at each variable node.

3. RLL-BCJR computes the extrinsic LLR for each bit and sends it as a priori information to the LDPC VND.

4. LDPC VND computes the messages to be sent to the LDPC CND using a priori information from the RLL-BCJR and the messages from the LDPC CND.

5. LDPC CND computes the extrinsic LLRs to be sent to the LDPC VND according to the LDPC code constraints.

6. LDPC VND computes the total LLRs for the input symbols and checks whether a valid codeword is obtained or not. Algorithm iterates until a valid codeword is obtained or a predetermined number of iterations are performed.

3.3 Outer LDPC Code Optimization

3.3.1 EXIT Chart Analysis

In order to optimize the decoding threshold of the concatenated RLL and LDPC coding scheme, we employ an EXIT chart analysis [56]. As it is introduced in the previous section, our iterative decoder consists of two blocks, denoted as Block A and Block B. We compute the mutual information at the output of each subblock and utilize the iterative decoder to draw the EXIT curves of different subblocks. By following the notation in [45], we denote the mutual information at the output of the LDPC VND and the LDPC CND by I_A and I_B, respectively, and the mutual information at the input and output of the RLL-BCJR block by I_V and I_S as depicted in Figure 3.3. We assume Gaussian distribution for the exchanged LLR values between the subblocks, hence we can use the low-complexity J function approximation to calculate I_A, I_B and I_V by the analytical formulas

$$I_A = \sum_i \lambda_i J\left(\sqrt{(i-1)(J^{-1}(I_B))^2 + (J^{-1}(I_S))^2}\right), \tag{3.8}$$

$$I_B = 1 - \sum_j \rho_j J\left(\sqrt{j-1}J^{-1}(1-I_A)\right), \tag{3.9}$$

$$I_V = \sum_i \lambda_i J\left(\sqrt{i}J^{-1}(I_B)\right), \tag{3.10}$$

where $\{\lambda_i\}$ and $\{\rho_j\}$ are the coefficients of variable and check node degree distributions $\lambda(x)$ and $\rho(x)$ that denote the fraction of the edges in the Tanner graph connected to degree-i variable nodes and degree-j check nodes, respectively [45], and J function is defined as

$$J(\sigma) = 1 - \int_{-\infty}^{\infty} \frac{1}{\sqrt{2\pi\sigma^2}} e^{-\frac{(x-\frac{\sigma^2}{2})^2}{2\sigma^2}} \log_2(1+e^{-x}) dx. \tag{3.11}$$

For computation of the mutual information at the output of the RLL-BCJR block (mutual information between the LLR values at the output of the RLL-BCJR decoder and the input symbols), we perform Monte Carlo simulations by taking a sufficiently long random input sequence. We model the a priori information of the RLL-BCJR algorithm by generating the input LLRs using the mutual information values from the LDPC VND, and the fact that the exchanged LLRs between the subblocks are normally distributed. Then, we calculate I_S as

$$I_S = I(L;X) \cong 1 - \frac{1}{N} \sum_{n=1}^{N} \log_2(1+e^{-L_n}), \tag{3.12}$$

where N is picked very large, and L_n denotes the LLR value of the nth coded bit of the all-zero codeword of length N. Note also that we utilize i.i.d. channel adapters [47] in our calculations since randomization of the all-zero sequence is required for the analysis.

3.3.2 Degree Distribution Optimization

LDPC codes that are optimized for P2P communication channels are not optimal when there is an inner code or modulation [45], in general, hence optimization of the degree distributions of the LDPC code ensembles may provide significant performance gains. Differential evolution and EXIT chart analyses are two common tools to optimize degree distributions of LDPC code ensembles. Here, we employ EXIT chart analysis due to its lower complexity to find optimal code ensembles.

In order to optimize the outer LDPC code, we fix the inner RLL code and optimize the decoding threshold of the LDPC code degree distribution. We compute the decoding threshold of an LDPC code ensemble by employing an EXIT

chart analysis, which is explained in the previous subsection in detail. A specific LDPC code ensemble is used if and only if the mutual information converges to 1, which demonstrates that the probability of error will vanish. If there exists a value I that satisfies $I_A(I) < I_B(I)$, then the tunnel between the EXIT curves of Block A and Block B is closed, i.e., iterative decoder does not converge and the probability of error cannot be made go to zero.

For the degree distribution optimization, we employ a random perturbation algorithm similar to the one in [45]. At each iteration of the optimization process, we perturb the degree distributions by zero-mean Gaussian random variables with a specific variance except for only three degrees, which are obtained by solving the following linear equations:

$$\sum_{i=1}^{\infty} \lambda_i = 1$$

$$\sum_{j=1}^{\infty} \rho_j = 1 \tag{3.13}$$

$$\sum_{j=1}^{\infty} \frac{\rho_j}{j} = (1-R) \sum_{i=1}^{\infty} \frac{\lambda_i}{i}. \tag{3.14}$$

where $0 \leq \lambda_i \leq 1$ and $0 \leq \rho_j \leq 1$. The last equation applies since the degree distributions should be compatible with the rate of the LDPC code.

After a new instance of a degree distribution is generated, we calculate the SNR threshold of the new degree distribution; if it is lower, we replace the degree distribution with the current one. The algorithm iterates until there is no improvement after a predetermined number of iterations.

3.4 Numerical Examples

In this section, we demonstrate the bit error rate performance of the designed codes for energy harvesting communication systems. We consider an energy harvester with an energy arrival probability of $q = 0.4$ and a unit-sized battery at the transmitter. We fix the inner code as the rate $\frac{2}{3}$ type-1 RLL(0,1) code. Note that the type-1 version of an RLL code can be obtained by switching the roles of ones and zeros [49]. The resulting ones density is $p = 0.27$. We compare the performance of three rate $\frac{1}{2}$ LDPC codes with block length $20k$: the first one is the regular (3,6) LDPC code, the second one is the irregular LDPC code optimized for an AWGN channel introduced in [57] with a maximum variable node degree of 4, and the third one is the LDPC code optimized for the specific inner RLL code and the energy harvesting process with multiple degrees of the variable and check nodes, and a maximum variable node degree 10. The resulting optimized degree distributions of the designed LDPC code are as follows:

$$\lambda_2 = 0.3070,\ \lambda_3 = 0.1868,\ \lambda_4 = 0.0607,\ \lambda_{10} = 0.4455,$$
$$\rho_5 = 0.4456,\ \rho_8 = 0.0580,\ \rho_{12} = 0.4964.$$

Performances of the three different codes are evaluated through finite block length simulations as depicted in Figure 3.4. The overall code rate is $\frac{1}{3}$. The results demonstrate that the newly optimized LDPC code yields a gain of approximately 0.55 dB compared to the LDPC code optimized over an AWGN channel, and 1.3 dB compared to regular (3,6) LDPC code at a bit error rate of 10^{-4}.

We evaluate the performance of the improved decoding approach by taking the optimized LDPC code for the type-1 RLL(0,1) code and evaluating its performance with the simplified and improved decoders through finite block length simulations. We take $q = 0.4$ and assume a unit-sized battery. Figure 3.5 depicts the corresponding results. We observe that the improved decoding approach is superior to the simplified one by approximately 0.6 dB at a bit error rate of 10^{-4} and it operates near the achievable rate limits (i.e., approximately within 0.9 dB).

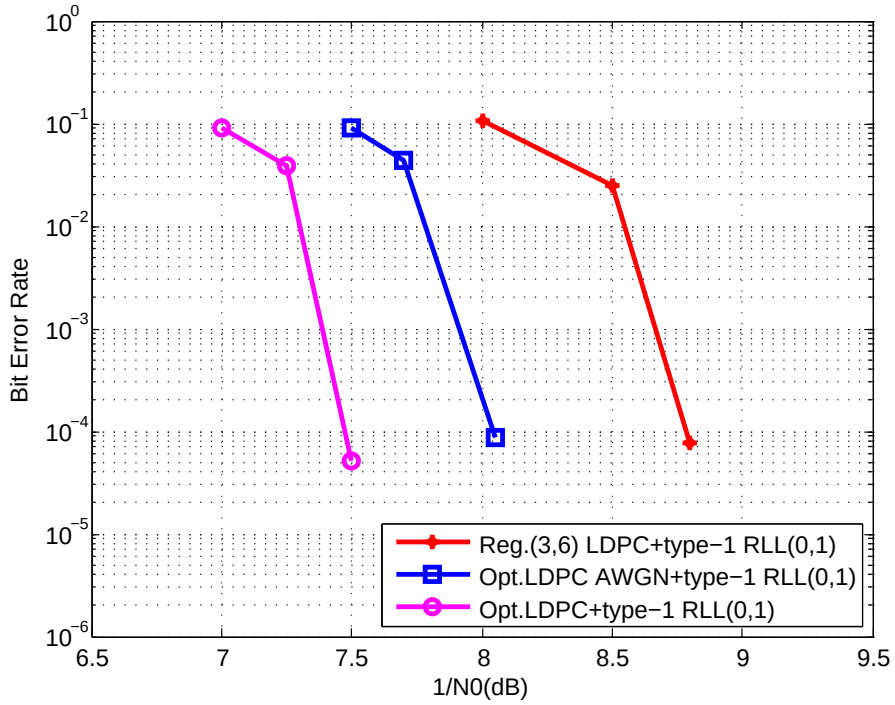

Figure 3.4: Bit error rate performance of three LDPC codes concatenated with rate R=$\frac{2}{3}$ type-1 RLL(0,1) code. Outer LDPC codes are of rate R=$\frac{1}{2}$ and block length 20k.

We emphasize that the advantage of using of the RLL codes with respect to the existing solutions based on NLTCs is that they allow us to obtain higher code rates compared to those obtained in [10]. In addition, our results are based on only 2-state RLL codes, which are very simple compared to the existing solutions.

3.5 Chapter Summary

In this chapter, we consider a binary energy harvesting communication system over an AWGN channel, and design practical codes. We exploit a serially concatenated coding scheme consisting of inner RLL and outer LDPC codes. At the receiver side, we employ an iterative decoder where a BCJR decoder matched to the RLL code and energy harvesting process exchanges extrinsic LLR values with an LDPC decoder. We consider two decoding approaches; while the simplified one ignores the memory in the battery state, the improved decoder exploits

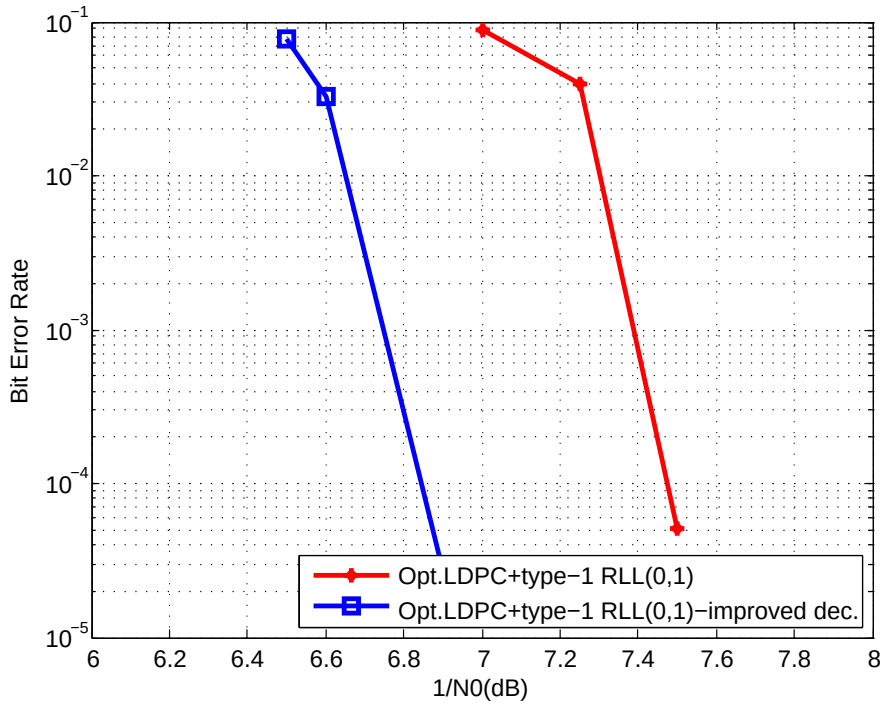

Figure 3.5: Bit error rate performance of optimized LDPC code concatenated with rate R=$\frac{2}{3}$ type-1 RLL(0,1) code with simplified and improved decoding. Block length of the LDPC code is 20k.

it. Since the optimized codes for P2P communications are not optimal for our scenario due to the existence of the inner code, we fix the inner RLL code and optimize the outer LDPC code by an EXIT chart analysis and a random perturbation technique. We demonstrate that our newly designed codes outperform the P2P optimal ones, and that the improved decoding approach is superior to the simplified one via numerical examples.

Chapter 4

Code Design for Joint Energy and Information Transfer with RLL Codes

In this chapter, our purpose is to design practical codes for joint energy and information transfer with the aim of increasing the transmitted energy levels as well as achieving reliable communication. Since classical linear block or convolutional codes induce a uniform input distribution at the channel input and a nonuniform input distribution is required to increase the transmitted energy levels, we utilize a serial concatenation of RLL and LDPC codes as in Chapter 3. For code design purposes, we fix the inner RLL code and design the outer LDPC code using the same procedure, and demonstrate that the newly optimized LDPC codes for the specific inner RLL code are superior to P2P optimal codes for joint information and power transfer.

The rest of the chapter is organized as follows. In Section 4.1, we describe the channel model and present information theoretic limits for joint energy and information transfer. In Section 4.2, we present the proposed solution. Numerical examples that illustrate the performance of the designed codes are the focus of Section 4.3, and the chapter is concluded in Section 4.4.

4.1 System Description

4.1.1 Channel Model

We consider transmission over an AWGN channel with the objective of joint energy and information transfer. The input-output relationship is given by

$$Y = X + Z \tag{4.1}$$

where $X \in \{0, 1\}$ is the channel input and Z is the Gaussian noise with zero mean and variance σ^2. We assume that the noise terms are i.i.d. across time. We consider on-off signalling to model the trade-off between the transmitted energy and the information rate assuming that $X = 1$ is an energy-carrying symbol and $X = 0$ carries no energy. Clearly, we can transmit more energy by transmitting codewords that have a higher ones density, however, this limits the information rates.

For the sake of joint energy and information transfer, the receiver has to harvest a certain level of energy. By assuming that an average ones density of p is required at the channel input, we employ RLL codes to induce this nonuniform input distribution. If the harvested energy per information bit at the receiver is p, the signal-to-noise ratio at the receiver side is defined as $\frac{E_b}{N_0} = \frac{p}{N_0}$.

4.1.2 Information Theoretic Limits

The mutual information between the input and output of an AWGN channel with an i.i.d. Bernoulli(p) distributed input is calculated as follows [48]:

$$I(X;Y) = h(Y) - \frac{1}{2} log(\pi e N_0) \tag{4.2}$$

where

$$h(Y) = -\int_{-\infty}^{\infty} f_Y(y) log(f_Y(y)) dy, \tag{4.3}$$

$$f_Y(y) = \frac{1}{\sqrt{\pi N_0}} \Big((1-p) e^{-\frac{y^2}{N_0}} + p e^{-\frac{(y-1)^2}{N_0}} \Big). \tag{4.4}$$

These equations illustrate that, in order to maximize the information rate, a ones density of $p = 0.5$ should be used at the channel input. However, in order to increase the transmitted power levels by increasing the ones density of the channel input, one should sacrifice some information rate.

4.2 Proposed Coding Scheme

We utilize a serially concatenated coding scheme as done in Chapter 3 with a small modification to adapt it for joint energy and information transfer. The block diagram of the transmitter and receiver is depicted in Figure 4.1. We employ an inner RLL code to make sure that the input has the desired distribution, and an outer LDPC code for error correction. The modification with respect to the proposed coding scheme in Chapter 3 is that the receiver is changed according to the absence of the energy harvesting process. Also, in this case, an RLL code inducing a ones density higher than 0.5 is employed to increase the transmitted power levels. The input message bits are encoded by an outer LDPC encoder and an inner RLL encoder, and then they are directly transmitted through an AWGN channel.

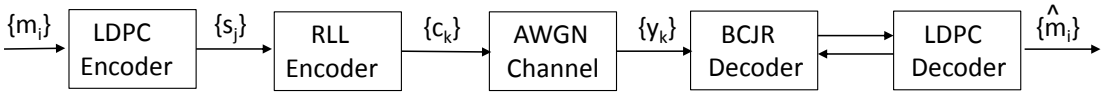

Figure 4.1: Block diagram of the transmitter, the channel and the iterative decoder.

At the receiver side, we employ an iterative decoder, i.e., the decoding is performed by exchanging extrinsic information between a BCJR decoder matched to the RLL code and an LDPC decoder. The main difference between the iterative decoder in Chapter 3 and the iterative decoder in this chapter is as follows. Since there is no energy harvesting process, the BCJR decoder is only matched to the RLL code, hence the LLR calculations at the output of the RLL-BCJR block are performed using [46]

$$L(u_l) = log\left[\frac{\sum\limits_{U^+} p(s_{l-1}=s', s_l=s, y)}{\sum\limits_{U^-} p(s_{l-1}=s', s_l=s, y)}\right], \tag{4.5}$$

$$p(s', s, y) = \alpha_{l-1}(s')\gamma_l(s', s)\beta_l(s), \tag{4.6}$$

$$\gamma_l(s', s) = \exp[u_k L^e(u_k)/2] \exp\left[-\frac{\|y_l - c_l\|^2}{2\sigma^2}\right], \tag{4.7}$$

where s_l is the encoder state at time l, U^+ is the set of state pairs (s', s) for which the state transitions are from state s' to state s with an encoder input of $u_l = 0$, and U^- is the set of state pairs (s', s) corresponding to $u_l = 1$. c_l is the corresponding codeword output for state transition (s', s), $L^e(u_k)$ is the a priori LLR of u_k, and y_l is the channel observation at time instance l.

Further details of the iterative decoding approach can be found in Chapter 3, and they are omitted here. We also note that, as in Chapter 3, the outer

LDPC code is optimized via a random perturbation algorithm and the convergence thresholds are computed using an EXIT chart analysis.

4.3 Numerical Examples

To illustrate the potential of the proposed scheme for joint energy and information transfer, we choose the rate $\frac{2}{3}$ RLL(0,1) code, which induces a ones density of $p = 0.73$. As in the energy harvesting case, we fix the inner RLL code and perform the code optimization over the degree distributions with a maximum variable node degree 10 for the outer LDPC code. The overall code rate of the concatenated coding scheme is $\frac{1}{3}$. The resulting optimized degree distribution is given by

$$\lambda_2 = 0.2885,\ \lambda_3 = 0.2947,\ \lambda_4 = 0.0023,\ \lambda_{10} = 0.4145,$$
$$\rho_5 = 0.4640,\ \rho_8 = 0.1147,\ \rho_{12} = 0.4213.$$

Performances of three different LDPC codes are evaluated through finite block length simulations, and they are depicted in Figure 4.2. The bit error rate simulations demonstrate that the optimized LDPC code for the inner RLL code is superior to the P2P optimized irregular LDPC code for AWGN channels by about 0.25 dB and to the regular LDPC code by about 0.6 dB at a bit error rate of 10^{-4}. The information theoretic limit for reliable communication at a transmission rate of $\frac{1}{3}$ for a ones density of $p = 0.73$ is at 5.3 dB, which means that our newly optimized codes are approximately 1.6 dB away from the theoretical limits of reliable communication.

We highlight that we can achieve a code rate of $\frac{1}{3}$ by utilizing an inner RLL code for joint energy and information transfer, which is higher than the one obtained in [9] (where the overall code rate of the communication scheme is $\frac{1}{6}$), for which the coding solution is based on the use of NLTCs.

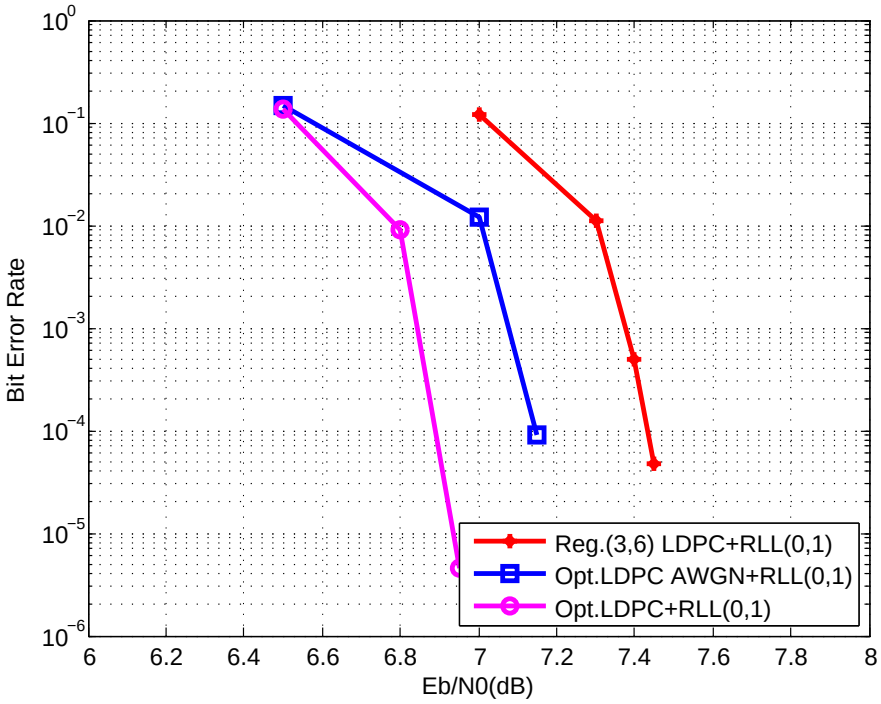

Figure 4.2: Bit error rate performance of three LDPC codes concatenated with RLL(0,1) code of rate $R = \frac{2}{3}$. Block lengths of the outer LDPC codes are $20k$ and $R = \frac{1}{2}$.

In addition, to demonstrate the superiority of the optimized LDPC codes designed for the specific inner RLL code compared to the P2P optimal LDPC codes, we consider the performance of our coding scheme with similar coding schemes in the literature. For this purpose, we consider the work in [9] for comparison, where a serial concatenation of an NLTC and an LDPC code is utilized for joint energy and information transfer. The overall code rate is $\frac{1}{6}$, hence we design rate $\frac{1}{4}$ LDPC codes to be used with the rate $\frac{2}{3}$ RLL(0,1) code. The optimized degree distribution of our code of rate $\frac{1}{4}$ is given by

$$\lambda_2 = 0.2837,\ \lambda_3 = 0.2174,\ \lambda_4 = 0.4989,$$
$$\rho_3 = 0.5814,\ \rho_4 = 0.1672,\ \rho_8 = 0.0329,\ \rho_{15} = 0.2185.$$

Figure 4.3 shows the bit error rate performances of the considered schemes. We note that there is a slight difference between the ones densities at the channel inputs of considered systems ($p = 0.73$ in our case and $p = 0.75$ in [9]), and this leads to a gap of about 0.34 dB in the required signal-to-noise ratio for a transmission rate of $\frac{1}{6}$. With this in mind, the performance results demonstrate

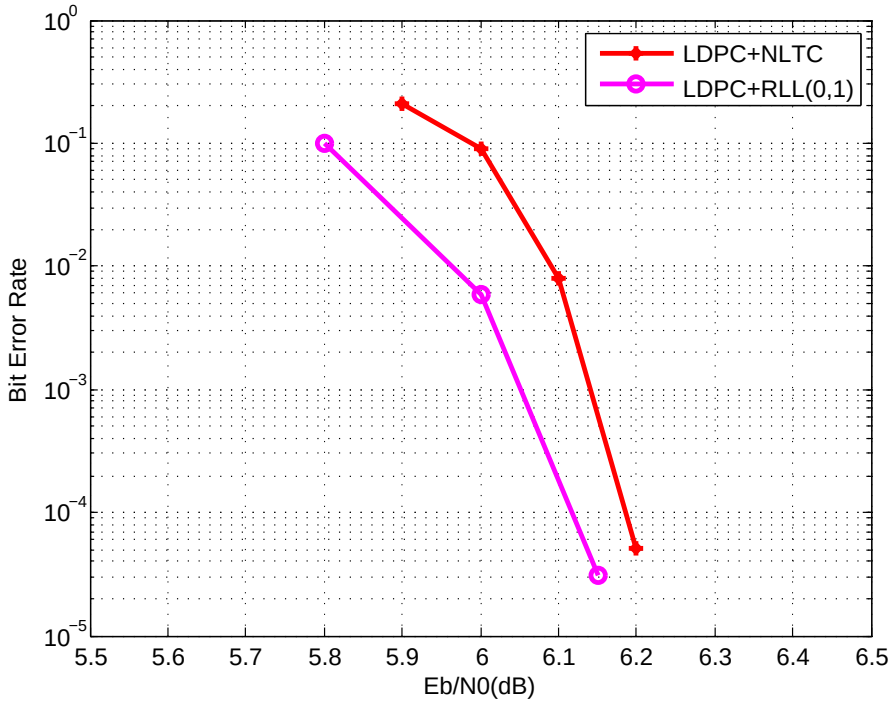

Figure 4.3: Performance comparison between the LDPC codes concatenated with NLTC and those concatenated with $R = \frac{2}{3}$ RLL(0,1) code ($R = \frac{1}{4}$, block length is $20k$).

that the proposed coding scheme offers competitive performance with the existing solutions.

4.4 Chapter Summary

In this chapter, we exploit the proposed coding scheme of concatenation of LDPC and RLL codes for joint energy and information transfer. The main idea is to increase the transmitted energy levels while achieving reliable communication. Therefore, we employ an inner RLL code that induces a ones density higher than 0.5 to obtain the nonuniform channel input along with an outer LDPC code. At the receiver side, a BCJR decoder matched to the RLL code exchanges soft information with an LDPC decoder to perform iterative decoding. Numerical examples demonstrate that the newly optimized LDPC codes are superior to P2P optimal codes, and they offer competitive performance with the existing solutions in the literature for the problem of joint energy and information transfer.

Chapter 5

Short Block Length Code Design for Energy Harvesting Communications and SWIPT using RLL Codes

While channel codes with asymptotically long block lengths lead to a close to capacity operation, they are not suitable for communication systems with stringent delay and complexity constraints, such as those to be employed in sensor networks. To satisfy the requirements of such systems, design of short block length codes is required. With this motivation, in this chapter, we consider an extension of our work in the previous two chapters to design short block length codes for energy harvesting communications and joint energy and information transfer.

The chapter is organized as follows. In Section 5.1, we introduce the system model. We describe the proposed coding scheme in Section 5.2 and the code design procedure in Section 5.3. We present several performance results of exemplary codes in Section 5.4, and conclude the chapter in Section 5.5.

5.1 System Model

We use the system models for energy harvesting communications and joint energy and information transfer introduced in Chapter 3 and Chapter 4 with small modifications. In particular, here, we propose to use RLL and convolutional codes in a serially concatenated manner. As in the long block length case, RLL codes are used to obtain a suitable non-uniform channel input distribution while, in this case, we employ convolutional codes as outer error correction codes instead of LDPC codes. Our motivation for not employing LDPC codes is based on the following: for very short block lengths, the codes' degree distributions do not exactly match the optimized ones, and their Tanner graphs include inevitable cycles, which degrade the iterative decoder performance [55], hence it may be preferable to pick trellis based coding solutions.

5.2 Proposed Coding Scheme

The proposed coding scheme for short block lengths is depicted in Figure 5.1, where the transmitter side includes a combination of a convolutional and RLL encoder. A possible way to encode with serial concatenation is as follows: encode the message sequence with the convolutional encoder, pass the coded bits to the RLL encoder through a random interleaver, and then encode the coded bits with the RLL encoder. However, since a random interleaver will cause problems in the decoding process, degrading the system performance, we omit it.

We describe the concatenated convolutional and RLL codes via a product trellis obtained by combining their state transitions. For example, for a 4-state convolutional code and a 2-state RLL code, where the states of the convolutional code are denoted as S_0, S_1, S_2, S_3, and the states of the RLL code are denoted as S'_0 and S'_1, the states of the concatenated convolutional and RLL codes can be represented as ordered pairs of the states of these two codes and they are denoted as $S_0S'_0$, $S_2S'_1$, etc. As an illustration, construction of the overall state diagram

and the product trellis for a (5,7) convolutional code (in octal notation) and an RLL(0,1) code are depicted in Figures 5.2 and 5.3, respectively.

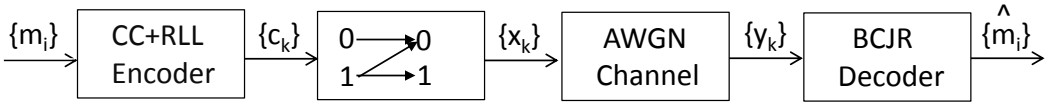

Figure 5.1: Block diagram of the proposed coding scheme.

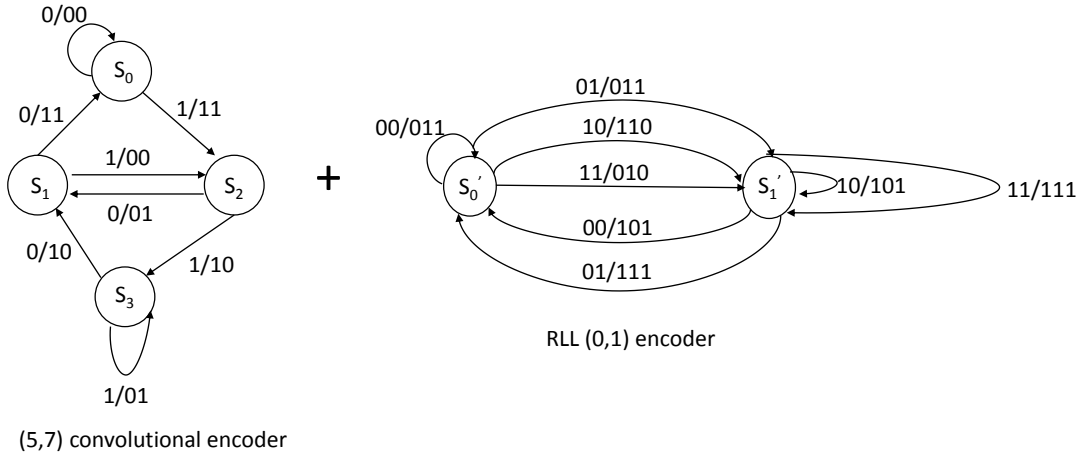

Figure 5.2: State transition diagrams of (5,7) convolutional and RLL(0,1) code.

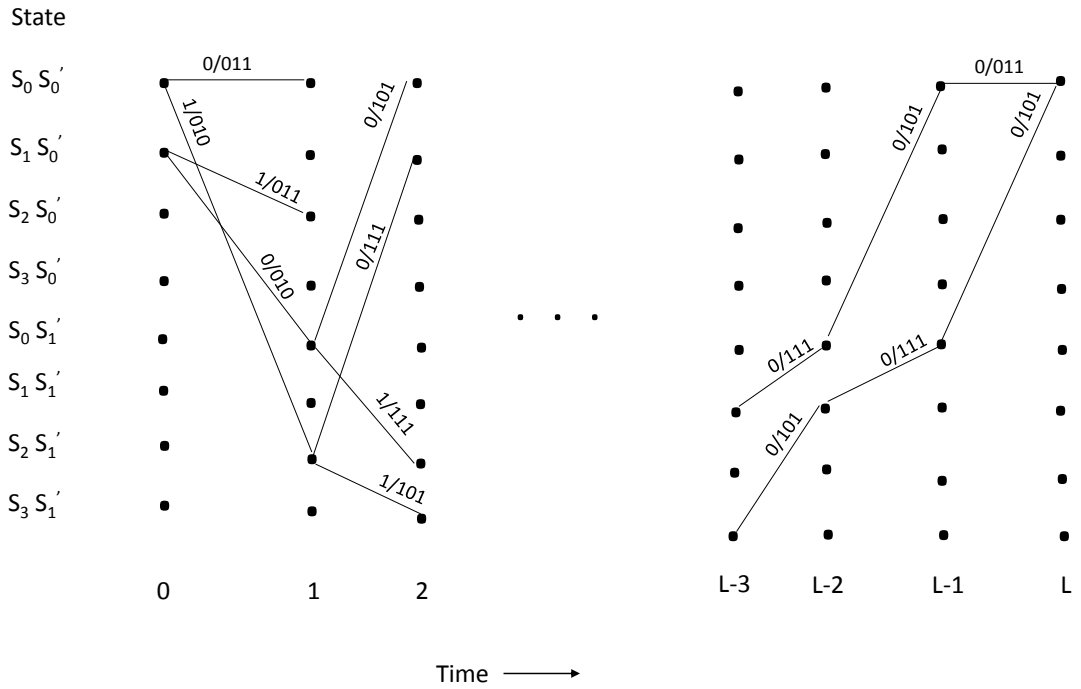

Figure 5.3: Product trellis representation of the concatenated code.

At the receiver side, decoding is performed via a BCJR algorithm operating on the product trellis. For simplicity, energy harvesting process is approximated as a Z-channel with $1 \to 0$ crossover probability is π_0 for the simplified decoding approach and it is directly embedded into the product trellis for the improved decoding solution for energy harvesting communications, as also done in Chapter 3.

We also employ the proposed coding scheme for joint energy and information transfer. In this case, there is no energy harvesting process, hence we do not need to match the BCJR decoder to it at the receiver side, and calculate the output LLR values as performed in the standard BCJR algorithm [46].

5.3 Code Design Procedure

We design specific codes by maximizing the minimum distance of the overall concatenated code. In order to determine the code's minimum distance, we compute the pairwise Hamming distance among all the codewords of the code with a sufficient number of stages in the trellis, making sure that the minimum pairwise Hamming distance among the considered length codewords gives the minimum distance of the overall code. We fix the RLL code, perform this procedure for all possible convolutional codes with a given memory order, and determine the non-catastrophic convolutional code when combined with the inner code that maximizes the minimum distance of the overall code as the optimal convolutional code.

5.4 Numerical Results

In this section, we present several examples to demonstrate the performance of the designed codes for energy harvesting communications and joint energy and information transfer. For both cases, we fix the inner RLL code and compare the performance of three convolutional codes. We also compare the performance of the designed concatenated codes with that of classical linear codes, used with time sharing for joint energy and information transfer.

As a first example, we compare the performance of a convolutional and an LDPC code concatenated with a type-1 RLL(0,1) code, where the block length is 48. We take the energy arrival probability as $q = 0.6$, and store the harvested energy in a battery of capacity 2. Figure 5.4 depicts the bit error rate performances of the considered schemes. We observe that the (5,7) convolutional code outperforms the optimized LDPC code for the specific inner RLL code by about 3 dB at a bit error rate of 10^{-3}. We argue that for very short block lengths, convolutional codes are superior to LDPC codes for error correction with energy harvesting, hence in the rest of the results we only consider the convolutional

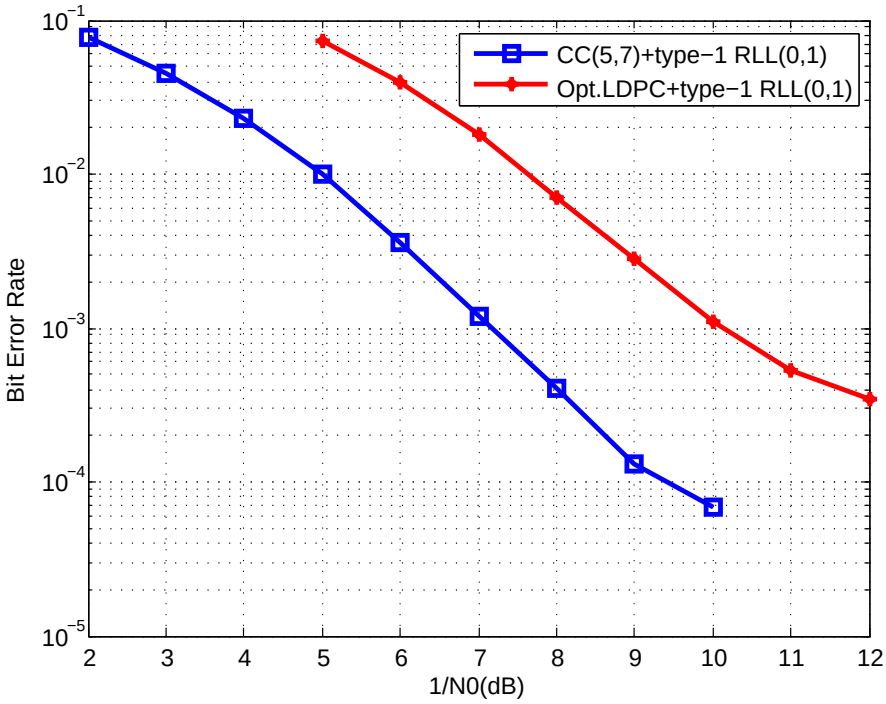

Figure 5.4: Bit error rate performance of concatenation of type-1 RLL(0,1) code with a convolutional or an LDPC code, where the block length is 48.

coding approach.

We now investigate the performance of convolutional codes in more depth. We utilize a type-1 RLL(0,1) code, which induces a ones density of $p = 0.27$ to obtain the required nonuniform input distribution for the energy harvesting process, and perform optimization over constraint length $k = 2$ convolutional codes. We take the energy arrival probability $q = 0.65$ and store the harvested energy in a battery of capacity 2.

We compare the concatenation of the three rate $\frac{1}{2}$ convolutional codes and a type-1 RLL(0,1) code. The convolutional codes are (5,7), (7,3) and (7,2) convolutional codes (expressed in octal notation). We note that the (5,7) convolutional code leads to a minimum distance of 4, the (7,3) code leads to a minimum distance of 3, and the (7,2) code leads to a minimum distance of 2 when concatenated with the type-1 RLL(0,1) code. We take the block length as 48, and depict the simulated bit error rate performances of these three codes in Figure 5.5. The results demonstrate that the (5,7) convolutional code outperforms the (7,3) code by about 1.2 dB and the (7,2) code by approximately 2.2 dB at a bit error rate

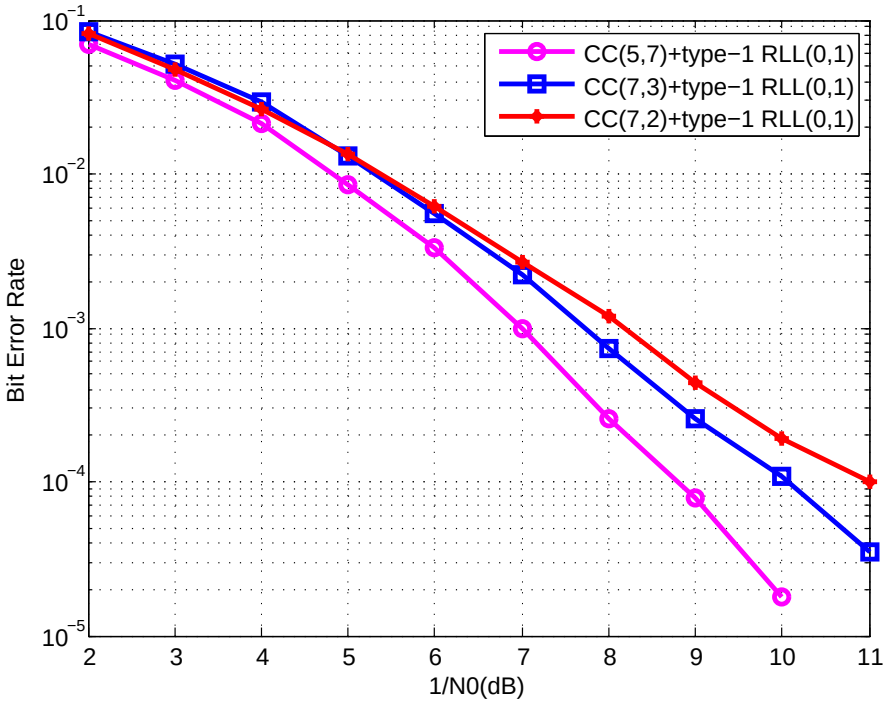

Figure 5.5: Bit error rate performance of three convolutional codes concatenated with rate $R = \frac{2}{3}$ type-1 RLL(0,1) code. Block length of concatenated codes is 48.

of 10^{-4}. We see that maximizing the minimum distance of the concatenated code leads to significant gains for energy harvesting.

As mentioned earlier, we also employ an improved decoder for the concatenated convolutional and RLL coding scheme by embedding the energy state into the product trellis. This is similar to what was done in Chapter 3 for energy harvesting communications. As an example, we take the concatenation of a (5,7) convolutional code and type-1 RLL(0,1) code, and compare the performance of this concatenated code decoded via simplified and improved decoders, assuming an energy arrival probability $q = 0.75$ and a unit-capacity battery. Figure 5.6 depicts the corresponding results, which demonstrate that the improved decoder is superior to the simplified decoder by about 0.75 dB at a bit error rate of 10^{-4}.

As another example, we compare the performance of the concatenated convolutional and RLL codes with that of a convolutional code alone. Specifically, we take the concatenation of the (5,7) convolutional code with the type-1 RLL(0,1) code as the concatenated coding solution, and the (13,15,17) convolutional code

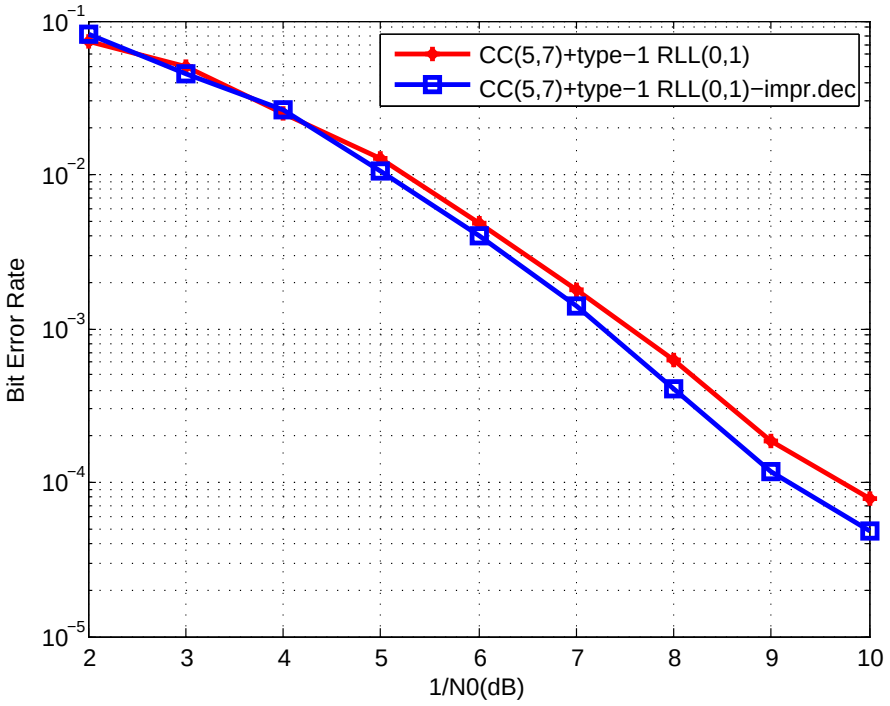

Figure 5.6: Bit error rate performance of concatenated code with simplified and improved decoder. Block length of concatenated code is 48.

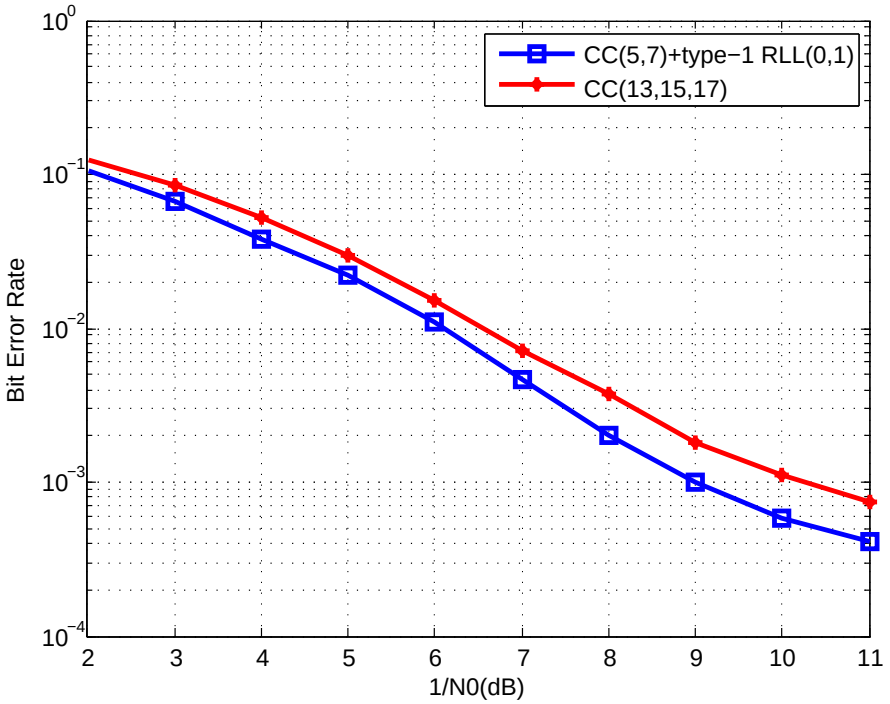

Figure 5.7: Bit error rate performance of concatenated code and convolutional code, where block length is 48 and $q = 0.6$.

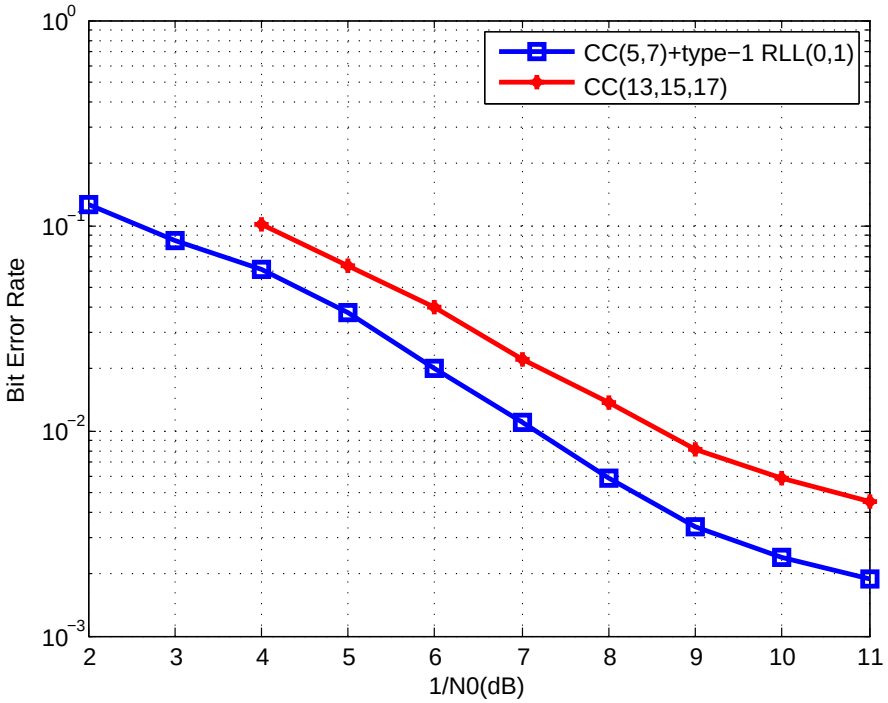

Figure 5.8: Bit error rate performance of concatenated code and convolutional code, where block length is 48 and $q = 0.5$.

for no code concatenation scenario to make sure that the code rate and the number of trellis states are the same. We consider two cases for the energy arrival probability: $q = 0.6$ and $q = 0.5$. In both cases, the harvested energy is stored in a unit-sized battery. Figures 5.7 and 5.8 depict the bit error rate performances of considered systems, demonstrating that the concatenated convolutional and RLL coding approach outperforms the convolutional code alone by about 1 dB at a bit error rate of 10^{-3} when $q = 0.6$, and by about 1.7 dB at a bit error rate of 10^{-2}, when $q = 0.5$. We observe that the performance gap between the concatenated convolutional and RLL coding approach and convolutional code alone increases as the energy arrival probability decreases. This is because the concatenated code suffers from reduced energy arrival rate less than a convolutional code alone due to its lower ones density at the channel input.

We also investigate the performance of the newly designed short block length codes for joint energy and information transfer. For this case, we employ an RLL(0,1) code to increase the transmitted power level, which induces a ones

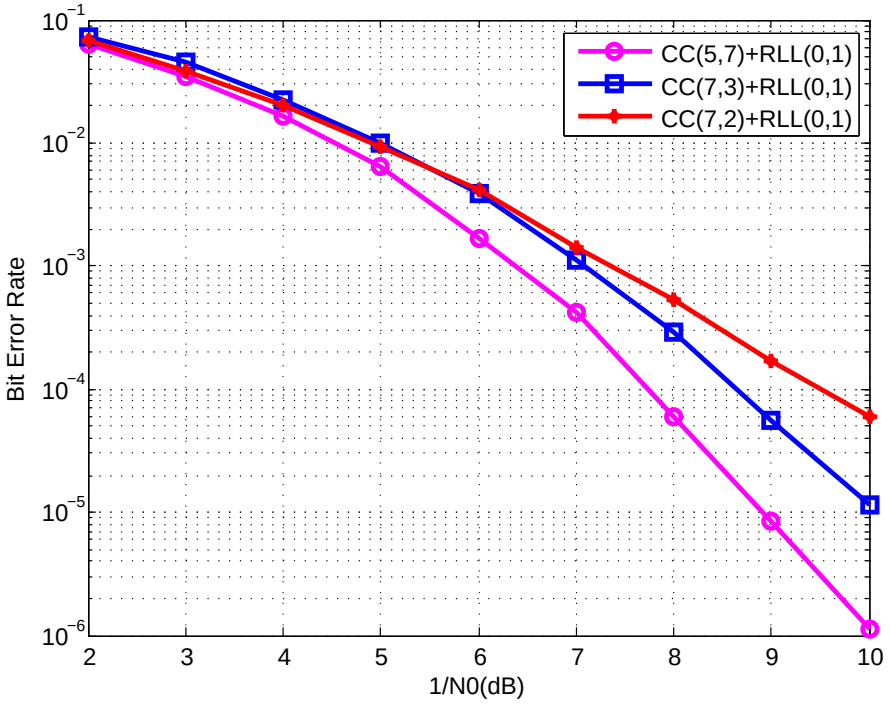

Figure 5.9: Bit error rate performance of three convolutional codes that are concatenated with rate $R = \frac{2}{3}$ RLL(0,1) code. Block length of concatenated codes are 48.

density of $p = 0.73$ at the channel input. For the design and selection of the concatenated codes, the same steps are followed with the energy harvesting case. Figure 5.9 depicts the resulting performances of the concatenated coding solutions. We observe that the (5,7) convolutional code, which offers a minimum distance of 4, provides a gain of 1 dB with respect to the concatenated code with the (7,3) convolutional code (with a minimum distance of 3), and 1.8 dB with respect to the (7,2) code, (with a minimum distance of 2) at a bit error rate of 10^{-4}.

As a final example, we compare performance of the designed concatenated codes with a convolutional code used with time switching for joint energy and information transfer. We consider the concatenation of (5,7) convolutional and RLL(0,1) codes among the newly designed codes, and the (15,17) convolutional code with no concatenation (with time switching), which offers the highest minimum distance among the convolutional codes with a constraint length of $k = 4$ for comparison. In order to use the convolutional code in the time switching mode,

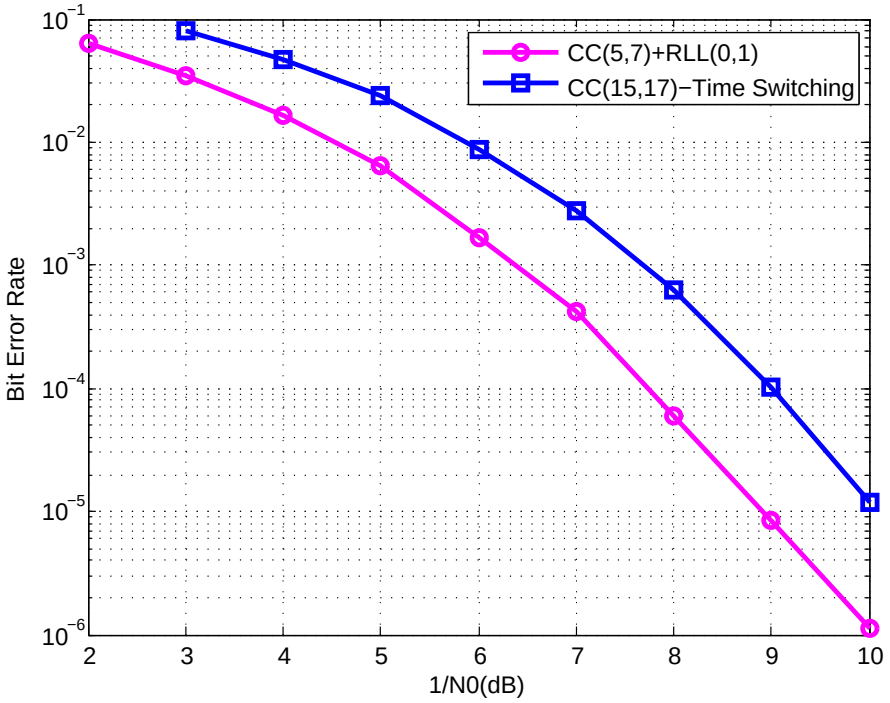

Figure 5.10: Bit error rate performance of short block length codes with rate R=$\frac{1}{3}$ and block length 48.

we send information and energy together half the time using on-off signalling and send only "1" in the other half, hence we have a ones density of $p = \frac{3}{4}$. Also, we puncture the convolutional code to satisfy the rate requirement for a fair comparison. Figure 5.10 demonstrates the performance of the designed concatenated and convolutional codes. We note that both the concatenated (5,7) convolutional and RLL(0,1) codes and the punctured (15,17) convolutional code have a minimum distance of 4. The results indicate that the newly designed code outperforms the convolutional code used in a time sharing mode by about 1.5 dB at a bit error rate of 10^{-4}. We attribute this improvement to the observation that the newly designed code includes less codeword pairs at the minimum distance of 4 than the punctured convolutional code (which was verified using MATLAB).

5.5 Chapter Summary

In this chapter, we focus on design of short block length codes for energy harvesting communications and joint energy and information transfer. As in the

previous chapters, we utilize RLL codes to obtain the required nonuniform input distribution. We employ convolutional codes for error correction instead of LDPC codes since the LDPC codes do not perform well for very short block lengths. We propose a coding scheme based on a serial concatenation of convolutional and RLL codes, and perform decoding via a BCJR algorithm over the product trellis of the convolutional and RLL codes at the receiver side. We design specific codes by maximizing the minimum distance of the concatenated code. Numerical examples illustrate that concatenated convolutional and RLL codes with higher minimum distances offer superior performance and they outperform the classical convolutional codes for joint information and energy transfer and energy harvesting communication scenarios.

Chapter 6

Conclusion and Future Work

In this thesis, we design practical codes for communications over noisy binary energy harvesting channels and joint energy and information transfer for both long block lengths (with the objective of approaching capacity limits) and short block lengths (where the target is communications with stringent delay and complexity requirements).

The proposed coding scheme consists of a serial concatenation of an inner RLL code and an outer LDPC code for the case of long block lengths. We first study energy harvesting communications where the encoded bits are transmitted through a noisy binary energy harvesting channel and a BCJR decoder matched to the RLL code and BEHC exchanges soft information with an LDPC decoder to perform iterative decoding at the receiver side. We consider two approaches for the iterative decoder: the simplified one ignores the memory in the battery state and the improved decoding approach integrates the battery state into the trellis. LDPC code design for the specific inner RLL code is based on an EXIT chart analysis and the random perturbation technique for optimization. We demonstrate the superiority of the newly designed codes to the LDPC codes optimized for point to point communications via numerical examples. We note that using of the RLL codes allows us to obtain higher code rates with respect to the existing solutions based on NLTCs.

As an extension of our work for energy harvesting, we also consider joint energy and information transfer. This is a highly related problem to energy harvesting communications and one can utilize the proposed coding scheme for energy harvesting communications with small modifications. In the case of joint energy and information transfer, the battery at the transmitter side is eliminated, hence the iterative decoder employs a BCJR decoder matched only to the RLL code. The design procedure of the outer LDPC code is the same as the one in the energy harvesting case. Numerical examples demonstrate that the optimized codes for the specific inner RLL code outperform the P2P optimal codes for this case as well.

We also examine design of the short block length codes for energy harvesting and joint energy and information transfer. We propose a serially concatenated coding scheme with an inner RLL code and an outer convolutional code, and describe the concatenated code via a product trellis. At the receiver side, decoding is performed via a BCJR algorithm over the product trellis representing the concatenated convolutional and RLL codes jointly. Specific codes are designed by maximizing the minimum distance of the overall code. Numerical examples illustrate that proposed short block length coding solutions with higher minimum distances offer superior performance.

We highlight several research directions as possible extensions of our work in this thesis. Here, we utilize 2-state RLL encoders taken from the previous literature. However, design of codes with memory that maximize the overall code's minimum distance while satisfying a specific ones density at the channel input may improve the performance. This has similarities with the design of NLTCs, however, we are after coding solutions with higher code rates and lower complexities. Also, in this thesis, we assume that causal information is available at the transmitter for the energy arrivals, however, different assumptions regarding the energy arrivals at both the transmitter and the receiver can also be considered. In addition, while we study the energy harvesting communications along with joint energy and information transfer over AWGN channels only, our work can be extended further to include different types of channels such as BSC or interference channels. Furthermore, the improved decoding approach can be utilized for

code design purposes possibly providing further gains. Finally, for the short block length case, we employ convolutional codes with a constraint length of only two, while designs with higher constraint lengths can also be considered to improve the system performance.

Bibliography

[1] X. Lu, P. Wang, D. Niyato, D. I. Kim and Z. Han, "Wireless networks with RF energy harvesting: A contemporary survey," *IEEE Commun Surv. Tuts*, vol. 17, no. 2, pp. 757-789, Second Quarter 2015.

[2] S. Ulukus, A. Yener, E. Erkip, O. Simeone, M. Zorzi, P. Grover and K. Huang, "Energy harvesting wireless communications: A review of recent advances," *IEEE Journal on Selected Areas in Communications*, vol. 33, no. 3, pp. 360-381, March 2015.

[3] K. Tutuncuoglu, O. Ozel, A. Yener and S. Ulukus, "The binary energy harvesting channel with a unit-sized battery," *IEEE Transactions on Information Theory*, vol. 63, no. 7, pp. 4240-4256, July 2017.

[4] O. Ozel and S. Ulukus, "Achieving AWGN capacity under stochastic energy harvesting," *IEEE Transactions on Information Theory*, vol. 58, no. 10, pp. 6471-6483, October 2012.

[5] O. Ozel and S. Ulukus, "AWGN channel under time-varying amplitude constraints with causal information at the transmitter," in *Proc. Record of the Forty Fifth Asilomar Conference of Signals, Systems and Computers*, Pacific Grove, CA, pp. 373-377, November 2011.

[6] V. Jog and V. Anantharam, "An energy harvesting AWGN channel with a finite battery," in *Proc. IEEE Symposium on Information Theory (ISIT)*, Honolulu, HI, pp. 806-810, August 2014.

[7] L. R. Varshney, "Transporting information and energy simultaneously," in *Proc. IEEE International Symposium on Information Theory (ISIT)*, Toronto, ON, pp. 1612-1616, July 2008.

[8] E. Zehavi and J. K. Wolf, "On runlength codes," *IEEE Transactions on Information Theory*, vol. 34, no. 1, pp. 45-54, January 1988.

[9] M. Dabirnia and T. M. Duman, "On code design for joint energy and information transfer," *IEEE Transactions on Communications*, vol. 64, no. 6, pp. 2677-2688, June 2016.

[10] M. Dabirnia and T. M. Duman, "Code design for binary energy harvesting channel," in *Proc. IEEE International Symposium on Information Theory (ISIT)*, Aachen, pp. 2345-2350, June 2017.

[11] C. E. Shannon, "Channels with side information at the transmitter," *IBM Journal*, pp. 289-293, October 1958.

[12] S. Verdu and T. S. Han, "A general formula for the channel capacity," *IEEE Transactions on Information Theory*, vol. 40, no. 4, pp. 1147-1157, July 1994.

[13] J. G. Smith, "The information capacity of amplitude and variance constrained scalar Gaussian channels," *Inf. Control*, vol. 18, no. 3, pp. 203-219, April 1971.

[14] W. Mao and B. Hassibi, "Capacity Analysis of Discrete Energy Harvesting Channels," *IEEE Transactions on Information Theory*, vol. 63, no. 9, pp. 5850-5885, September 2017.

[15] P. Castiglione, O. Simeone, E. Erkip and T. Zemen, "Energy management policies for energy-neutral source-channel coding," *IEEE Transactions on Communications*, vol. 60, no. 9, pp. 2668-2678, September 2012.

[16] C. Tapparello, O. Simeone and M. Rossi, "Dynamic compression-transmission for energy-harvesting multihop networks with correlated sources," *IEEE/ACM Transactions on Networking*, vol. 22, no. 6, pp. 1729-1741, December 2014.

[17] O. Orhan, D. Gunduz and E. Erkip, "Delay-constrained distortion minimization for energy harvesting transmission over a fading channel," in *Proc. IEEE International Symposium on Information Theory (ISIT)*, Istanbul, pp. 1794-1798, July 2013.

[18] F. C. Schoute, "Dynamic frame length ALOHA," *IEEE Transactions on Communications*, vol. 31, no. 4, pp. 565-568, April 1983.

[19] F. Ianello, O. Simeone, and U. Spagnolini, "Medium access control protocols for wireless sensor networks with energy harvesting," *IEEE Transactions on Communications*, vol. 60, no. 5, pp. 1381-1389, May 2012.

[20] C. K. Ho and R. Zhang, "Optimal energy allocation for wireless communications with energy harvesting constraints," *IEEE Transactions on Signal Processing*, vol. 60, no. 9, pp. 4808-4818, September 2012.

[21] O. Ozel, K. Tutuncuoglu, J. Yang, S. Ulukus and A. Yener, "Transmission with energy harvesting nodes in fading wireless channels: Optimal policies," *IEEE Journal on Selected Areas in Communications*, vol. 29, no. 8, pp. 1732-1743, September 2011.

[22] W. Li, Z. Nan, X. Wang and X. Zhou, "Optimal transmission policy for energy-harvesting powered MIMO multi-access channels," in *Proc. IEEE/CIC ICCC 2014 Symposium on Selected Topics in Communications*, Shanghai, pp. 286-291, October 2014.

[23] K. Wu, C. Tellambura and H. Jiang, "Optimal transmission policy in energy harvesting wireless communications: A learning approach," in *Proc. IEEE ICC 2017 Ad-Hoc and Sensor Networking Symposium (ICC)*, Paris, pp. 1-6, May 2017.

[24] A. Zanella, A. Bazzi, B. M. Massini and G. Pasolini, "Optimal transmission policies for energy harvesting nodes with partial information of energy arrivals," in *Proc. IEEE 24th International Symposium on Personal, Indoor and Mobile Radio Communications: Fundamentals and PHY Track (PIMRC)*, London, pp. 954-959, September 2013.

[25] A. Ozcelikkale, T. McKelvey and M. Viberg, "Transmission strategies for remote estimation with an energy harvesting sensor," *IEEE Transactions on Wireless Communications*, vol. 16, no. 7, pp. 4390-4403, July 2017.

[26] A. Ozcelikkale, T. McKelvey and M. Viberg, "Performance bounds for remote estimation with an energy harvesting sensor," in *Proc. IEEE International Symposium on Information Theory (ISIT)*, Barcelona, pp. 460-464, July 2016.

[27] L. P. Qian, G. Feng and V. C. M. Leung, "Optimal transmission policies for relay communication networks with ambient energy harvesting relays," *IEEE Journal on Selected Areas in Communications*, vol. 34, no. 12, pp. 3754-3768, December 2016.

[28] J. Yang and J. Wu, "Optimal transmission for energy harvesting nodes under battery size and usage constraints," in *Proc. IEEE International Symposium on Information Theory (ISIT)*, Aachen, pp. 819-823, June 2017.

[29] K. Huang, "Spatial throughput of mobile ad hoc networks powered by energy harvesting," *IEEE Transactions on Information Theory*, vol. 59, no. 11, pp. 7597-7612, November 2013.

[30] K. Huang, M. Kountouris and V. O. K. Li, "Renewable powered cellular networks: Energy field modeling and network coverage," *IEEE Transactions on Wireless Communications*, vol. 14, no. 8, pp. 4234-4247, August 2015.

[31] P. Popovski, A. M. Fouladgar and O. Simeone, "Interactive joint transfer of energy and information," *IEEE Transactions on Communications*, vol. 61, no. 5, pp. 2086-2097, May 2013.

[32] P. Grover and A. Sahai, "Shannon meets Tesla: Wireless information and power transfer," in *Proc. IEEE International Symposium on Information Theory (ISIT)*, Austin, TX, pp. 2363-2367, June 2010.

[33] X. Zhou, R. Zhang and C. K. Ho, "Wireless information and power transfer: Architecture design and rate-energy tradeoff," *IEEE Transactions on Communications*, vol. 61, no. 11, pp. 4754-4767, November 2013.

[34] R. Zhang and C. K. Ho, "MIMO broadcasting for simultaneous wireless information and power transfer," *IEEE Transactions on Wireless Communications*, vol. 12, no. 5, pp. 1989-2001, May 2013.

[35] J. Xu, L. Liu and R. Zhang, "Multiuser MISO beamforming for simultaneous wireless information and power transfer," *IEEE Transactions on Signal Processing*, vol. 62, no. 18, pp. 4798-4810, September 2014.

[36] X. Xu, A. Ozcelikkale, T. McKelvey and M. Viberg, "Simultaneous information and power transfer under a non-linear RF energy harvesting model," in *Proc. ICC2017: WS02-IEEE Workshop on Emerging Energy Harvesting Solutions for 5G Networks (5G-NRG)*, Paris, pp. 179-184, May 2017.

[37] A. Ozcelikkale, T. McKelvey and M. Viberg, "Simultaneous information and power transfer with transmitters with hardware impairments," in *Proc. International Symposium on Wireless Communication Systems (ISWCS)*, Poznan, pp. 114-118, September 2016.

[38] L. Liu, R. Zhang and K. - C. Chua, "Wireless information transfer with opportunistic energy harvesting," *IEEE Transactions on Wireless Communications*, vol. 12, no. 1, pp. 288-300, January 2013.

[39] J. Park and B. Clerckx, "Joint wireless information and energy transfer in a two-user MIMO interference channel," *IEEE Transactions on Wireless Communications*, vol. 12, no. 8, pp. 4210-4221, August 2013.

[40] Z. Ding, S. M. Perlaza, I. Esnaola and H. V. Poor, "Simultaneous information and power transfer in wireless cooperative networks," in *Proc. 8th International Conference on Communications and Networking in China (CHINACOM)*, Guilin, pp. 252-256, August 2013.

[41] A. Ozcelikkale and T. M. Duman, "Linear precoder design for simultaneous information and energy transfer over two-user MIMO interference channels," *IEEE Transactions on Wireless Communications*, vol. 14, no. 10, pp. 5836-5847, October 2015.

[42] A. Ozcelikkale, T. McKelvey and M. Viberg, "Wireless information and power transfer in MIMO channels under Rician fading," in *Proc. IEEE International Conference on Acoustics, Speech and Signal Processing (ICASSP)*, Brisbane, QLD, pp. 3187-3191, April 2015.

[43] J. Zhang, C. Yuen, C. - K. Wen, S. Jin, K. - K. Wong and H. Zhu, "Large system secrecy rate analysis for SWIPT MIMO wiretap channels," *IEEE Transactions on Information Forensics and Security*, vol. 11, no. 1, pp. 74-85, January 2016.

[44] J. - M. Kang, I. - M. Kim and D. I. Kim, "Joint optimal mode switching and power adaptation for nonlinear energy harvesting SWIPT system over fading channel," *IEEE Transactions on Communications*, vol. 66, no. 4, pp. 1817-1832, April 2018.

[45] M. Francheschini, G. Ferrari and R. Raheli, "Serial concatenation of LDPC codes and differential modulations," *IEEE Journal on Selected Areas in Communications*, vol. 23, no. 9, pp. 1758-1768, September 2005.

[46] W. E. Ryan and S. Lin, "Channel codes: Classical and modern," *Cambridge, U.K.: Cambridge Univ. Press.*, 2009.

[47] J. Hou, Paul H. Siegel, L. B. Milstein and H. D. Pfister, "Capacity-approaching bandwidth-efficient coded modulation schemes based on low-density parity check codes," *IEEE Transactions on Information Theory*, vol. 49, no. 9, pp. 2141-2155, September 2003.

[48] T. M. Cover and J. A. Thomas, "Elements of information theory," *2nd ed.*, New York, NY, USA, Wiley 2006.

[49] A. M. Fouladgar, O. Simeone and E. Erkip, "Constrained codes for joint energy and information transfer," *IEEE Transactions on Communications*, vol. 62, no. 6, pp. 2121-2130, June 2014.

[50] A. Tandon, M. Motani and L. R. Varshney, "On code design for simultaneous energy and information transfer," *Information Theory and Applications Workshop*, San Diego, CA, pp. 2356-2362, February 2014.

[51] A. Tandon, M. Motani and L. R. Varshney, "Subblock-constrained codes for real-time simultaneous energy and information transfer," *IEEE Transactions on Information Theory*, vol. 62, no. 7, pp. 4212-4227, July 2016.

[52] S. Arimoto, "An algorithm for computing the capacity of the arbitrary discrete memoryless channels," *IEEE Transactions on Information Theory*, vol. 18, no. 1, pp. 14-20, January 1972.

[53] R. E. Blahut, "Computation of channel capacity and rate-distortion functions," *IEEE Transactions on Information Theory*, vol. 18, no. 4, pp. 460-473, July 1972.

[54] C. Wang and M. Motani, "Coding for the binary energy harvesting channel with finite battery," in *Proc. IEEE Information Theory Workshop (ITW)*, Kaohsiung, pp. 554-558, November 2017.

[55] S. Sharifi, M. Dabirnia, A. K. Tanc and T. M. Duman, "Short block length code design for interference channels," in *Proc. IEEE International Symposium on Information Theory (ISIT)*, Barcelona, pp. 1909-1913, July 2016.

[56] S. ten Brink, "Convergence behaviour of iteratively decoded parallel concatenated codes," *IEEE Transactions on Communications*, vol. 49, no. 10, pp. 1727-1737, October 2001.

[57] T. J. Richardson, M. A. Shokrollahi and R. L. Urbanke, "Design of capacity-approaching irregular low-density parity check codes," *IEEE Transactions on Information Theory*, vol. 47, no. 2, pp. 619-637, February 2001.